BER Modeling for Interference Canceling Adaptive NLMS Equalizer

Tamoghna Roy

Thesis submitted to the Faculty of the
Virginia Polytechnic Institute and State University
in partial fulfillment of the requirements for the degree of

Master of Science
In
Electrical Engineering

A. A. (Louis) Beex, Chair
Jeffrey H. Reed
Douglas K. Lindner

December 1, 2014

Blacksburg, VA

Keywords: (N)LMS Equalizer, Non-Wiener Effects, BER Modeling, Gaussian Mixture Model

© 2014 Tamoghna Roy

BER Modeling for Interference Canceling Adaptive NLMS Equalizer

Tamoghna Roy

ABSTRACT

Adaptive LMS equalizers are widely used in digital communication systems for their simplicity in implementation. Conventional adaptive filtering theory suggests the upper bound of the performance of such equalizer is determined by the performance of a Wiener filter of the same structure. However, in the presence of a narrowband interferer the performance of the LMS equalizer is better than that of its Wiener counterpart. This phenomenon, termed a non-Wiener effect, has been observed before and substantial work has been done in explaining the underlying reasons. In this work, we focus on the Bit Error Rate (BER) performance of LMS equalizers.

At first a model – the Gaussian Mixture (GM) model – is presented to estimate the BER performance of a Wiener filter operating in an environment dominated by a narrowband interferer. Simulation results show that the model predicts BER accurately for a wide range of SNR, ISR, and equalizer length. Next, a model similar to GM termed the Gaussian Mixture using Steady State Weights (GMSSW) model is proposed to model the BER behavior of the adaptive NLMS equalizer. Simulation results show unsatisfactory performance of the model. A detailed discussion is presented that points out the limitations of the GMSSW model, thereby providing some insight into the non-Wiener behavior of (N)LMS equalizers. An improved model, the Gaussian with Mean Square Error (GMSE), is then proposed. Simulation results show that the GMSE model is able to model the non-Wiener characteristics of the NLMS equalizer when the normalized step size is between 0 and 0.4. A brief discussion is provided on why the model is inaccurate for larger step sizes.

Dedicated to my grandparents:

Late Mr. Asitesh Chandra Roy
Mrs. Manjusree Roy
Late Mr. Ranendranath Mitra
Late Mrs. Purnima Mitra

ACKNOWLEDGEMENTS

I am grateful to my advisor, Dr. A. A. (Louis) Beex for his help, support and encouragement through the course of my graduate studies at Virginia Tech. His guidance along with his profound knowledge in Signal Processing paved the way for this research. His continual mentorship and engaging interactions not only helped me learn how to conduct research efficiently but also, how to present it effectively and aesthetically.

I also want to reach out to my other committee members - Dr. Jeffrey H. Reed and Dr. Douglas K. Linder and acknowledge them for their time and valuable feedback.

Pursuing higher education in USA would not have been possible without the relentless support I had from my mother – Mrs. Sanchita Roy. This thesis substantiates her sustained faith in my abilities, which motivated me to overcome obstacles and strive to better myself, each day. My father – Mr. Amitava Roy, for those endless conversations on myriad topics ranging from politics to the weather which allowed me to feel connected to home, even though I was away. My sister – Ms. Titas Roy, budding dentist, who kept me well versed with medical jargon – for her observations and critique which kept me grounded.

Sreyoshi Bhaduri – thank you for making me write those 'two pages' and for those numerous trips to Starbucks, coaxing me to finish up. This thesis, along with many other things, would not have been the same without you.

I want to express my gratitude to the teachers of my undergraduate classes – Dr. Amitava Chatterjee and Professor Sugato Munshi, for introducing me to this wonderful discipline of signal processing. Additionally, my alma-mater – Jadavpur University – for those glorious four years which shaped me.

I am lucky to have a few people whom I can call friends – Debayan, Debsubhra, Gourab, Poulomi, Neil, Nirmalya, Subhabrata, Debarshi – thank you for the endless banters and the productive distractions.

Lastly, I would like to mention three very special people who have had a significant influence on me – Dr. Debasis Barman, for introducing and nurturing my interest in Mathematics. Dr. Sunanda Mitra, for setting the foundation for my graduate research in the US. Dr. Santanu Das, for believing in my capabilities even before I myself was cognizant of them, thank you for the constant motivation and continual guidance without which I would not have been able to pursue this adventure called ‘grad school’.

TABLE OF CONTENTS

LIST OF FIGURES

LIST OF TABLES

CHAPTER 1 INTRODUCTION

This chapter provides the necessary background for this work and sets up the research problem. A brief background regarding adaptive equalization and narrowband interference is presented first, followed by a literature review highlighting the relevant works that dealt with the non-Wiener characteristics of the adaptive LMS class of equalizers. The contribution of this work to the domain of the problem is summarized in Section 1.3. Lastly, Section 1.4 contains the mapping for the remaining thesis.

1.1 Background

Adaptive Equalizers are an integral part of any digital communication system. For a majority of practical situations the channel conditions are not known a priori. Moreover, the channel conditions may be time varying. Adaptive Equalizers provide a solution to this problem by compensating for the channel impairments and in case of time varying channels, adapting to the time varying channel response [1].

To our best knowledge, Adaptive Equalization for digital communication systems was first proposed by Lucky [2]. His work was based on minimizing the peak distortion criterion. Concurrently, Widrow et al. [3] devised the Least Mean Square (LMS) algorithm which was computationally simple and converged to the optimal Wiener solution. Proakis and Miller [4] showed an adaptive receiver based on the LMS algorithm which was capable of adjusting to the unknown slowly time varying channel conditions. An excellent summary of adaptive equalization techniques is presented by Qureshi [5].

The primary objective of an equalization technique is to undo the unwanted effect of the channel characteristic – inter-symbol interference on the received communication signal. Although Qureshi [5] mentions that any technique employed to reduce inter-symbol interference can be considered an equalization technique, equalization can be viewed in general as a mitigation technique. In this work, our focal point will be

modeling the performance of digital communication systems where narrowband interference has been suppressed by Adaptive Equalizers; more specifically by Adaptive LMS or NLMS Equalizers.

Narrowband interference and its mitigation has been a topic of a great deal of research since this type of interference corrupts the desired signal in numerous systems. These narrowband interferences can be intentional like narrowband jamming in tactical communications. In some cases, the narrowband interference is unintentional like the power line interference in ECG signals. Irrespective of the cause of origin it is desirable to get rid of this interference.

There has been a substantial amount of work regarding suppression of narrowband interference. Milstein [6] in his work gives a brief summary of methods of rejecting interference in spread spectrum communication systems emphasizing primarily two schemes – 1. LMS based and 2. Transform domain processing structure based. Laster and Reed [7] provide a comprehensive survey of interference rejection methods for both spread spectrum and non-spread spectrum communication systems. Poor [8] gives a detailed account of various interference mitigation schemes based on different techniques, such as linear predictive methods, non-linear predictive methods, linear code aided methods, etc. Batra [9] examines the effect of severe narrowband interference on a wireless communication system and proposes two novel methods - 1. Data-aided Initialization (DAI) and 2. Two stage filtering, which utilizes a prediction error filter (PEF) as a pre-filter to the equalizer, for faster convergence of the adaptive equalizer weights.

Adaptive LMS equalizers were seen to behave ‘unconventionally’ in the presence of a narrowband interference, as was first observed by North, Axford, and Zeidler [10]. The term ‘unconventional’ demands special attention.

Conventional adaptive filtering suggests the Wiener filter as the appropriate benchmark against which the performance of the adaptive filter is measured [11]. In this work we are interested in LMS equalizers for which the Wiener equalizer is considered to provide the lower bound since the LMS algorithm is subject to misadjustment error due

to weight adaptation. For this reason, traditionally LMS equalizers are implemented with small step sizes. North, Axford, and Zeidler [10] observed that the performance of LMS equalizers was superior in terms of probability of error to that of the corresponding Wiener equalizer with the same structure in an environment dominated by narrowband interference. This effect will be referred to as a non-Wiener characteristic of adaptive LMS equalizers. The next section gives a brief review of the work done regarding non-Wiener characteristics of LMS equalizers.

1.2 Literature Review

As mentioned earlier, the non-Wiener characteristics of adaptive equalizers were first observed by North, Axford, and Zeidler [10]. Reuter and Zeidler [12] demonstrated that the steady state Mean Square Error (MSE) of LMS equalizers can better the corresponding Wiener equalizer of the same structure. This work also tries to model the non-linear nature of the LMS algorithm and quantify the MSE performance of the LMS algorithm. However, the experimental results and the theoretical results did not coincide, pointing to limitations in the model. In subsequent works [13-15], it has been shown that LMS may outperform the corresponding Wiener filter and the performance is dependent on system parameters such as Signal to Noise Ratio (SNR), Signal to Interference Ratio (SIR), length of the equalizer, and the adaptation step size.

Beex and Zeidler [16] modeled the interference canceller as a two channel Wiener Filter with the interference signal as the input to the second channel. This work showed that the adaptive NLMS filter is trying to track a time-varying target solution. This two-channel model was extended to Recursive Least Squares (RLS) adaptation [17] and adaptive noise cancellation [18].

Conventional adaptive filtering theory posits that the steady state weights for LMS equalizers converge to the corresponding Wiener weights. Ikuma, Beex, and Zeidler [19] derived a closed form expression for the mean of the LMS weight vectors in steady state. The expression was derived from the Butterweck expansion of the weight update

equation [20]. Simulation results were in conformity with the analytical results for all step-sizes where the expansion converges. In a subsequent work [21], it was shown that the analytical solution holds true over a wide range of ISR.

Reuter and Zeidler [12] first proposed a transfer function based approach to quantify the MSE performance of LMS equalizers. The results were inaccurate since the model assumed that the mean of the LMS weights in steady state converged to the corresponding Wiener weights which as shown in [19, 21] is not true. Hence, the Reuter-Zeidler model for the MSE was not an accurate one. Ikuma and Beex [22] incorporate the shift in the mean of the steady state weights and proposed a new model for MSE. Simulation results illustrate the improvement of the new model over the previous Reuter-Zeidler model. The derivations for the mean LMS weights in steady state and the improved MSE model have been excellently documented [23].

In this thesis, we are interested in formulating a model predicting the Bit Error Rate (BER) behavior of the adaptive LMS equalizers in an environment contaminated by a strong narrowband interference. The BER serves as a more practical metric to measure the performance of a digital communication system than MSE. Surprisingly, very little literature exists which deals with this particular topic.

North, Axford, and Zeidler [10] compared the performances of different adaptive equalizers in terms of probability of error. However, the error probability was computed via simulation and no model was proposed.

Prior to this, Iltis and Milstein [24] provided a statistical analysis of the LMS algorithm where the adaptive filter was used to suppress a fading gone jammer. The work provided a BER model which inherently assumes slow convergence (i.e. a near Wiener case) and a large equalizer length. In this thesis, we are primarily interested in large step sizes where the non-Wiener characteristics are predominant. A Gaussian BER approach was also adopted [25]. However, no simulation results were provided to support the claims.

Coulson [26] investigates the effect of narrowband interference on OFDM systems. An analytical Gaussian model is provided to gauge the effect of the narrowband interference on receiver post detection BER performance. However, no analytical model is put forward to estimate the BER post interference suppression. Instead a heuristic method to estimate the BER is provided where the latter is simply the ensemble median of the simulation results.

1.3 Contributions

The primary contribution of this thesis is analyzing the superior BER performance of the LMS equalizer compared to its Wiener counterpart. There has been very little work in the area of developing BER models, as reviewed in Section 1.2. This thesis attempts to explain the reason behind the superior BER performance and proposes models that will estimate or model the BER performance of an LMS equalizer in a narrowband interference dominated environment.

Secondly, this thesis presents a model to describe the BER performance of the Wiener equalizer operating in a narrowband interference dominated environment. Simulation results show that the model is very accurate over a wide range of SNR and SIR. This Wiener BER model provides a benchmark for comparing the BER performance of the LMS equalizer. This model also highlights the significant difference between the adaptive and the fixed case thereby helping us in gaining a better understanding of the non-Wiener behavior of the LMS equalizers.

1.4 Organization

The thesis is comprised of three main chapters. Before analyzing the adaptive case, we analyze the BER performance of the Wiener filter in an environment dominated by narrowband interference in Chapter 2. The chapter includes a detailed derivation of the BER model and simulation results. In Chapter 3, a BER model similar to the one proposed in Chapter 2 is applied to the adaptive NLMS case. Simulation results and a

detailed discussion analyzing the results are provided. Chapter 4 contains a new BER model for the adaptive NLMS case. Simulations showing the comparison of the different models are provided, followed by a discussion. Finally, concluding remarks and future directions are provided in Chapter 5.

CHAPTER 2 BER MODELING FOR FIR WIENER EQUALIZER

Wiener Filtering theory provides the analytical expression for the Mean Square Error (MSE). However, for practical communication systems Bit Error Rate (BER) is frequently used as a metric for system performance as well as an indicator of Quality of Service (QoS). While mean squared error (MSE) is assumed to relate to bit error rate (BER), the connection between the two performance metrics is not necessarily a direct one when the detector output noise is not Gaussian. We show that BER can be increasing for increasing signal power (or decreasing noise power) even though MSE is decreasing; this occurrence is counter-intuitive. The expression for the BER when the receiver output is Gaussian is pretty well known. In this chapter we consider a system which is corrupted by narrowband interference and then proceed towards developing statistical model(s) which can predict the BER of the system. The performance of the models is compared to simulation results.

2.1 FIR Wiener Equalizer

Figure 2-1 shows the block diagram of the system under consideration. The symbols transmitted at time instant n are denoted by d_n, while i_n and n_n respectively denote the sinusoidal interference and the zero-mean AWGN (additive, white, Gaussian noise). Thus, the input process to the Wiener equalizer is given by:

$$x_n = d_n + i_n + n_n \tag{2.1}$$

which is seen to be a summation of three independent wide sense stationary (WSS) processes.

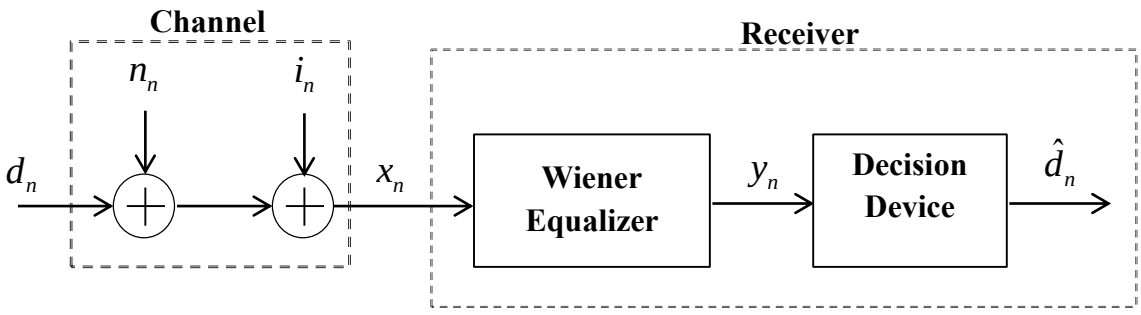

Figure 2-1. Block Diagram of the Wiener Equalizer System.

Let $\mathbf{w} = \begin{bmatrix} w_1 & w_2 & \cdots & w_L \end{bmatrix}^T$ be the vector of FIR Wiener filter weights, and $\mathbf{x}_n = \begin{bmatrix} x_n & x_{n-1} & \cdots & x_{n-L+1} \end{bmatrix}^T$ be the vector input to the Wiener filter at time *n*; with *T* denoting the transpose operator. The output of the Wiener filter at time *n* is then given by:

$$\begin{aligned} y_n &= \mathbf{w}^{\mathbf{H}}\mathbf{x}_n \\ &= \mathbf{w}^{\mathbf{H}}\mathbf{d}_n + \mathbf{w}^{\mathbf{H}}\mathbf{i}_n + \mathbf{w}^{\mathbf{H}}\mathbf{n}_n \\ &= y_n^d + y_n^i + y_n^n \end{aligned} \tag{2.2}$$

where H denotes the Hermitian transpose operator, and the other definitions follow the vector convention above. The FIR Wiener filter is found by solving the Wiener-Hopf equation [11]

$$\mathbf{R}_{\mathbf{x}}\mathbf{w} = \mathbf{p} \tag{2.3}$$

with the definitions: $\mathbf{R}_{\mathbf{x}} \triangleq E\left\{\mathbf{x}_n\mathbf{x}_{\mathbf{n}}^{\mathbf{H}}\right\}$ and $\mathbf{p} \triangleq E\left\{\mathbf{x}_n d_{n-\Delta}^*\right\}$. The resulting minimum MSE is then given by [11]

$$MMSE = \sigma_d^2 - \mathbf{w}^H\mathbf{p} \tag{2.4}$$

From (2.3) we can see that in the narrowband interference canceling environment, the FIR Wiener weights will be dependent on the fractional interference frequency f_i as the term $\mathbf{R}_{\mathbf{x}}$ is a function of f_i which is later shown in Section 2.4.

2.2 Gaussian Mixture Model

To evaluate BER performance, the PDF of y_n conditioned on $d_{n-\Delta}$ (usually $\Delta = (L-1)/2$, the "center" of equalization, but the point of equalization can actually be any value/location) is needed for each of the possible symbol values the latter can take on. As a result of independence, and the Wiener filter being linear time invariant (LTI), the right-hand side components in (2.2) can be evaluated separately in terms of the corresponding mean and variance.

2.2.1 Conditional PDF of y_n^n

The AWGN is independent of the symbol sequence and the interference, so that this output component does not depend on the conditioning symbol. A linear combination of independent Gaussian random variables produces a Gaussian random variable [27]. So in order to completely describe the PDF of y_n^n we need to evaluate its mean and variance. Note that, as we are working at baseband, the zero-mean AWGN is assumed to be circularly symmetric, with real and imaginary parts that are independent and identically distributed.

The mean of y_n^n is derived in (2.5):

$$\begin{aligned} E\left(y_n^n\right) &= E\left\{\mathbf{w}^{\mathbf{H}}\mathbf{n}_n\right\} \\ &= E\left\{\sum_{i=1}^{L} w_i^* n_{n-i+1}\right\} \\ &= \sum_{i=1}^{L} w_i^* E\left\{n_i\right\} = 0 \end{aligned} \tag{2.5}$$

and the variance of y_n^n is derived in (2.6):

$$
\begin{aligned}
Var\left(y_n^n\right) &= Var\left\{\mathbf{w}^{\mathbf{H}}\mathbf{n}_n\right\} \\
&= Var\left\{\sum_{i=1}^{L} w_i^* n_{n-i+1}\right\} \\
&= \sum_{i=1}^{L} Var\left\{w_i^* n_{n-i+1}\right\} \\
&= \sum_{i=1}^{L} \left|w_i\right|^2 Var\left\{n_n\right\} \\
&= \sum_{i=1}^{L} \left|w_i\right|^2 \sigma_n^2 \\
&= \left\|\mathbf{w}\right\|_2^2 \sigma_n^2
\end{aligned}
\tag{2.6}
$$

where σ_n^2 is the input noise power and $\left\|.\right\|_2$ denotes the Euclidean norm. As a result, the PDF of y_n^n is given by:

$$
y_n^n \sim CN\left(\mathbf{0}, \left\|\mathbf{w}\right\|_2^2 \sigma_n^2\right) \tag{2.7}
$$

where, $\chi \sim CN(\mu, 2\sigma^2)$ indicates that χ is a complex normal random variable, or a real vector random variable with mean $\mu = \begin{bmatrix} \mathrm{Re}\left\{E(\chi)\right\} \\ \mathrm{Im}\left\{E(\chi)\right\} \end{bmatrix}$ and covariance $\begin{bmatrix} \sigma^2 & 0 \\ 0 & \sigma^2 \end{bmatrix}$.

2.2.2 Conditional PDF of y_n^d

Let the modulation scheme have M symbols denoted by $\left\{\phi_m\right\}_{m=1}^{\mathrm{M}}$, so that the conditional PDF of interest is $f\left(y_n^d \middle| d_{n-\Delta} = \phi_m\right)$. Note that this fixes the "equalization-point" component in $\mathbf{d}_n$, which is multiplied by the corresponding element of the weight vector, say w_Δ, while the L-1 remaining terms in (2.8) produce a sum of random variables, i.e.

$$
\begin{aligned}
y_n^d\Big|_{d_{n-\Delta}=\phi_m} &= \sum_{l=0}^{L-1} w_l^* \phi_k \\
&= w_\Delta^* \phi_m + \sum_{\substack{l=0 \\ l\neq\Delta}}^{L-1} w_l^* \phi_k
\end{aligned}
\tag{2.8}
$$

The first term on the right-hand-side is deterministic, while the symbols under the sum are random and independent. In addition assuming a modulation scheme such that the mean of all possibilities in the constellation is zero, we can then evaluate mean:

$$
\begin{aligned}
E\left[y_n^d \middle| d_{n-\Delta} = \phi_m \right] &= E\left[w_\Delta^* \phi_m + \sum_{\substack{l=0 \\ l\neq\Delta}}^{L-1} w_l^* \phi_k \right] \\
&= E\left[w_\Delta^* \phi_m \right] + E\left[\sum_{\substack{l=0 \\ l\neq\Delta}}^{L-1} w_l^* \phi_k \right] \\
&= w_\Delta^* \phi_m + \sum_{\substack{l=0 \\ l\neq\Delta}}^{L-1} E\left[w_l^* \phi_k \right] \\
&= w_\Delta^* \phi_m + \sum_{\substack{l=0 \\ l\neq\Delta}}^{L-1} w_l^* E\left[\phi_k \right] \\
&= w_\Delta^* \phi_m
\end{aligned}
\tag{2.9}
$$

The variance can be computed by:

$$
\begin{aligned}
Var\left[y_n^d \middle| d_{n-\Delta} = \phi_m \right] &= Var\left[w_\Delta^* \phi_m + \sum_{\substack{l=0 \\ l\neq\Delta}}^{L-1} w_l^* \phi_k \right] \\
&= Var\left[w_\Delta^* \phi_m \right] + Var\left[\sum_{\substack{l=0 \\ l\neq\Delta}}^{L-1} w_l^* \phi_k \right] \\
&= \sum_{\substack{l=0 \\ l\neq\Delta}}^{L-1} Var\left[w_l^* \phi_k \right] = \sum_{\substack{l=0 \\ l\neq\Delta}}^{L-1} \left| w_l \right|^2 Var\left[\phi_k \right] \\
&= \sigma_\phi^2 \sum_{\substack{l=0 \\ l\neq\Delta}}^{L-1} \left| w_l \right|^2
\end{aligned}
\tag{2.10}
$$

where σ_ϕ^2 is the symbol power. Each of the terms under the sum in (2.8) contributes a PDF (actually a PMF or probability mass function) corresponding to a symbol constellation that is rotated and scaled, by w_i given by:

$$w_l\phi_k \sim \frac{1}{M}\sum_{m=1}^{M}\delta\left(x - w_l\phi_m\right) \tag{2.11}$$

The various terms under the sum in (2.8) are independent, so that the overall PMF is given by the convolution of the various PMFs of the form in (2.11). The resulting conditional PDF is therefore:

$$\begin{aligned} f\left(y_n^d \middle| d_{n-n_0} = \phi_m\right) &= \frac{1}{M^{L-1}} \sum_{k_1,\cdots,k_{L-1}=1}^{M} \delta\left(x - \mu_{m\mathbf{k}}\right) \\ \mu_{m\mathbf{k}} &= w_j\phi_m - \sum_{l=1,\neq j}^{L-1} w_l\phi_{k_i} \end{aligned} \tag{2.12}$$

Figure 2-2 shows an example to illustrate the PDF described in (2.12). For our example we used the QPSK modulation scheme so that $M = 4$. The filter length L is taken to be 3 and the interference frequency $f_i = 1/e$. The PDF has $M^{L-1} = 16$ discrete values which are equally likely. This result is consistent with (2.12).

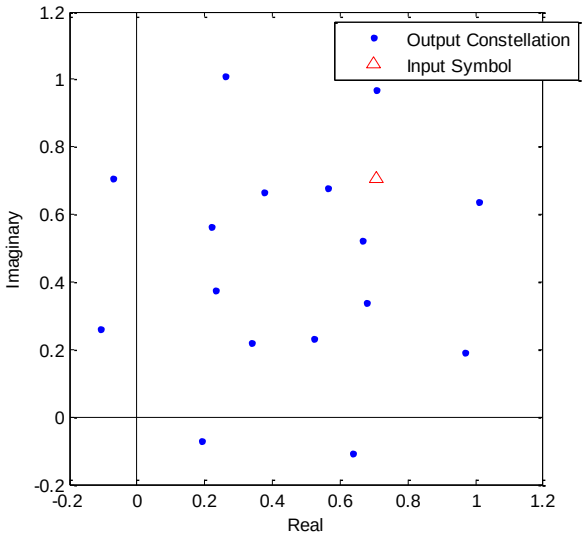

Figure 2-2. Output Constellation Map for QPSK with L = 3 and f_i=1/e .

2.2.3 Conditional PDF of y_n^i

The additive zero-mean sinusoidal interference is given by:

$$i_n = \sigma_i e^{j(\omega_i n+\theta)} \tag{2.13}$$

where σ_i^2 is the average power, $\omega_i = 2\pi f_i$ is the fractional angular frequency, and θ is the random phase. θ is uniformly distributed in the interval $[0, 2\pi)$ radians but is fixed for each realization. The random phase makes it a WSS process [27].

The interference is independent of the transmitted symbol sequence. The interference process described in (2.13) follows an Arc-Sine distribution [27] and thus the PDF of y_n^i also follows the same distribution as a LTI system (in this case FIR Wiener equalizer) only shifts and scales the input sinusoid. However, for ease of analysis we will assume that the latter follows a Gaussian distribution. The implications of this assumption will be discussed in Section 2.4.

Under the assumption that y_n^i follows a Gaussian distribution we need to find the mean and the variance to describe the PDF completely.

The mean of y_n^i is derived in (2.14):

$$\begin{aligned} E(y_n^i) &= E\left\{\mathbf{w^H i_n}\right\} \\ &= E\left\{\sum_{k=1}^{L} w_k^* i_{n-k+1}\right\} \\ &= \sum_{k=1}^{L} w_k^* E\left\{i_n\right\} \\ &= 0 \end{aligned} \tag{2.14}$$

and the variance of y_n^i is derived in (2.15):

$$
\begin{aligned}
Var\left[y_n^i \right] &= Var\left[\mathbf{w^H i_n} \right] \\
&= E\left[\left(\mathbf{w^H i_n} \right) \left(\mathbf{w^H i_n} \right)^H \right] \\
&= E\left[\mathbf{w^H i_n i_n^H w} \right] \\
&= \mathbf{w^H} E\left[\mathbf{i_n i_n^H} \right] \mathbf{w} \\
&= \mathbf{w^H R_i w}
\end{aligned}
\tag{2.15}
$$

with the definitions: $\mathbf{R_i} \triangleq \sigma_i^2 e^{j\omega_i n_0} \boldsymbol{\xi}\boldsymbol{\xi}^{\mathbf{H}}$ and $\boldsymbol{\xi} \triangleq [1 \quad e^{-j\omega_i} \quad \cdots \quad e^{-j\omega_i (M-1)}]^T$. $\mathbf{R_i}$ is the auto-correlation matrix for the input sinusoidal process.

Thus, the PDF of the interference component process y_n^i is given by:

$$
y_n^i \sim CN\left(\mathbf{0}, \mathbf{w^H R_i w} \right) \tag{2.16}
$$

The Wiener filter aims to minimize MSE. Thus in an interference dominated environment (large interference to signal ratio (ISR)) the interference gets pretty much canceled, because it provides the largest contribution to MSE. As a result, the residual interference component y_n^i is negligible in comparison with the other two components contributing to the Wiener filter output. Under such conditions, the variance computed in (2.15) can be neglected.

2.2.4 Conditional PDF of y_n

The noise component, the signal component, and the interference component of the LTI Wiener filter output are independent, so that the overall conditional PDF of y_n is the convolution of the corresponding PDFs, i.e. the convolution of the results in (2.7), (2.12), (2.16) which is a Gaussian Mixture (GSM) model.

$$f\left(y_n \middle| d_{n-\Delta} = \phi_m\right) \cong \frac{1}{M^{L-1}} \sum_{k_1,\cdots,k_{L-1}=1}^{M} CN\left(\mu_{m\mathbf{k}}, \|\mathbf{w}\|_2^2 \sigma_n^2 + \mathbf{w}^{\mathbf{H}}\mathbf{R}_{\mathbf{i}}\mathbf{w}\right)$$
$$\mu_{m\mathbf{k}} = w_\Delta \phi_m - \sum_{\substack{l=1 \\ l\neq\Delta}}^{L-1} w_l \phi_{k_i} \tag{2.17}$$

For an interference dominated environment the GM model is written without taking into account the contribution from the interference component.

$$f\left(y_n \middle| d_{n-\Delta} = \phi_m\right) \cong \frac{1}{M^{L-1}} \sum_{k_1,\cdots,k_{L-1}=1}^{M} CN\left(\mu_{m\mathbf{k}}, \|\mathbf{w}\|_2^2 \sigma_n^2\right)$$
$$\mu_{m\mathbf{k}} = w_\Delta \phi_m - \sum_{\substack{l=1 \\ l\neq\Delta}}^{L-1} w_l \phi_{k_i} \tag{2.18}$$

Based on the conditional PDF model in (2.17) or (2.18), we can calculate the probability of bit-error by evaluating the volume enclosed by the complex normal distribution in the regions corresponding to a bit error. The regions are determined by the modulation scheme used and the choice of decision boundaries.

For example, for the QPSK modulation scheme as used in the subsequent simulations, a received symbol is detected as a first quadrant symbol if both the in-phase and quadrature component are positive. If the transmitted symbol is in the first quadrant the probability of bit error (P_e) is evaluated by computing the volume enclosed by each of the complex normal distributions in (2.17) in the second, third, and fourth quadrant. The volume enclosed in the third quadrant is multiplied by 2 (as the third quadrant implies that both bits are in error) before being added to the contributions from the second and fourth quadrant. Then that final sum is divided by the factor M^{L-1} which is the probability associated with each of the terms in the GM model.

2.3 Gaussian Model

To improve the BER performance of a communication system, longer equalizers are generally used. With an increase in the length of the equalizer the number of discrete

points in $f\left(y_n^d \middle| d_{n-\Delta} = \phi_m\right)$ increases exponentially as the number of points in the output constellation is given by M^{L-1}. As a result, the number of individual Gaussians in (2.16) or (2.17) also increases. Therefore the Gaussian sum model becomes computationally expensive.

Figure 2-3 shows the output constellation for an equalizer length of L = 10, which gives rise to 262,144 Gaussian distribution terms compared to 16 terms for L = 3 (shown in Figure 2-2). While there are clearly non-Gaussian features, it seems reasonable to approximate this fairly circular probability mass with its best Gaussian fit. So for larger values of L we propose an approximated version of the Gaussian Mixture model, consisting of a single Gaussian term.

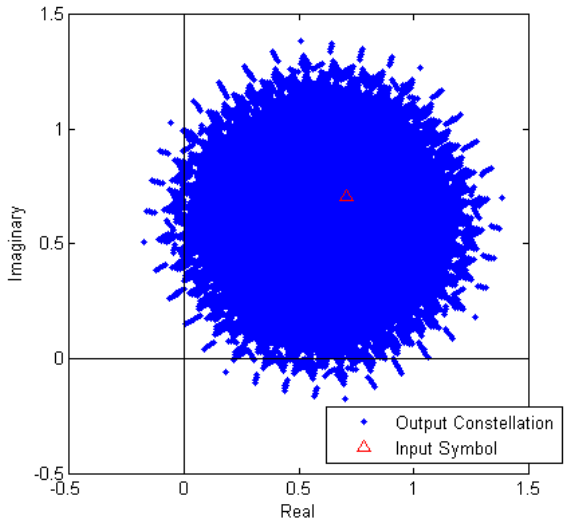

Figure 2-3. Output Constellation for QPSK with L = 10 and f_i=1/e .

2.3.1 Conditional PDF of y_n

The Gaussian model assumes the PDF of the conditional output $f\left(y_n \middle| d_{n-\Delta} = \phi_m\right)$ to follow a Gaussian distribution. The mean of this distribution is the same as that derived

in (2.9) and the variance is given by the sum of the variances described in (2.7), (2.10) and (2.15). Thus, the Gaussian model PDF is given by:

$$f\left(y_n \middle| d_{n-\Delta}=\phi_m\right) \sim CN\left(w_\Delta \phi_m, \|\mathbf{w}\|_2^2 \sigma_n^2 + \sum_{\substack{l=0 \\ l\neq\Delta}}^{L-1} |w_l|^2 \sigma_\phi^2 + \mathbf{w}^{\mathbf{H}}\mathbf{R}_{\mathbf{i}}\mathbf{w}\right) \tag{2.19}$$

Following arguments as for the GM model, for an interference dominated environment we can neglect the interference component and (2.19) can be re-written as:

$$f\left(y_n \middle| d_{n-\Delta}=\phi_m\right) \sim CN\left(w_\Delta \phi_m, \|\mathbf{w}\|_2^2 \sigma_n^2 + \sum_{\substack{l=0 \\ l\neq\Delta}}^{L-1} |w_l|^2 \sigma_\phi^2\right) \tag{2.20}$$

We use the PDF characterized in (2.20) to then model the probability of bit error for the Gaussian model.

2.4 Frequency Effect

The frequency of the interference signal evaluated from (2.3) impacts system performance. A change in interference frequency alters the Wiener weights. The changed Wiener weights in turn will affect the output constellation. To show this we use similar conditions used to generate Figure 2-2 only changing the interference frequency from $1/e$ to $1/4e$.

With the change in interference frequency we see a rotation in the output constellation. However, the number of discrete points is still $M^{L-1}=16$. This result is also consistent with (2.12).

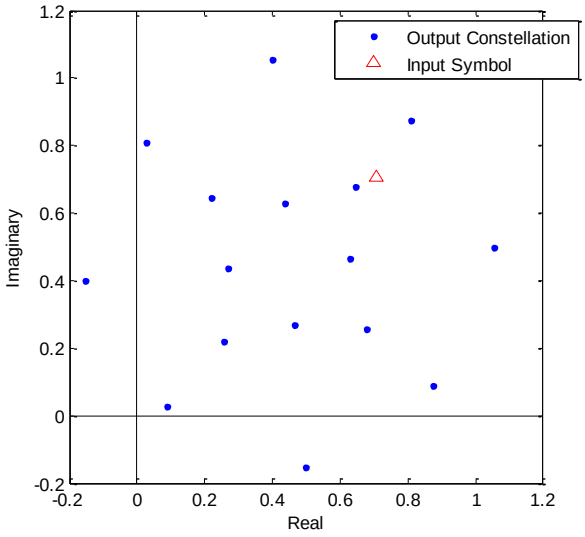

Figure 2-4. Output Constellation Map for QPSK with L = 3 and f_i =1/4e.

2.5 Simulation Results

In the simulation example, we look into a communication system that employs QPSK modulation, i.e. $M = 4$, and for which the average over all constellation values equals zero. The QPSK signal is corrupted by a narrowband interference (represented by a complex sinusoid) and zero mean additive white Gaussian noise. The signal, interference, and noise are all wide sense stationary and independent processes with known statistics, so that the Wiener filter is LTI and its MSE performance can be readily evaluated, according to (2.4).

Figure 2-5 shows the MSE performance of the communication system for a Wiener equalizer of length $L = 3$ for two different situations: when there is no narrowband interference at all and when there is strong narrowband interference (ISR = 20 dB), and for the two different interference frequencies of $f_i = 1/e$ and $f_i = 1/4e$.

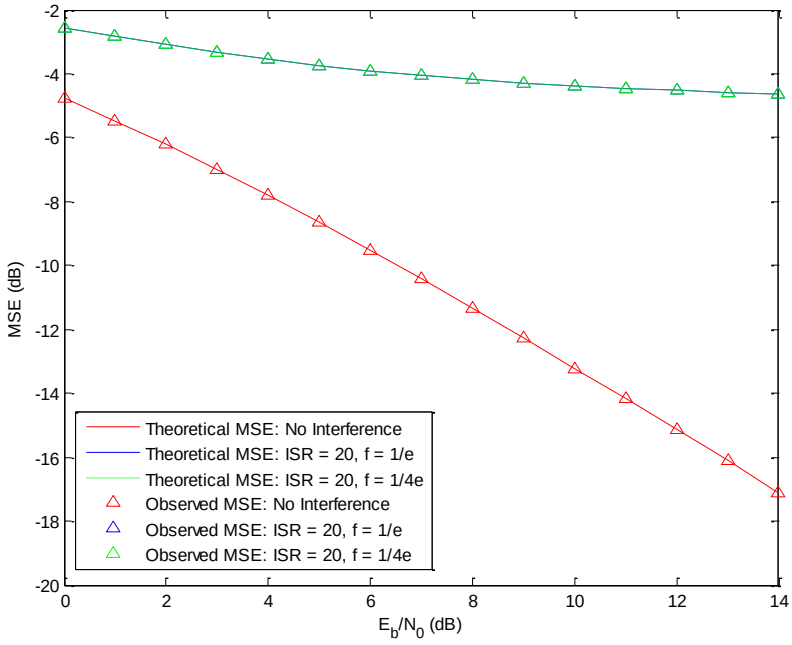

Figure 2-5. MSE performance for L = 3.

It is to be noted that for all cases the MSE performance is monotonically decreasing with a decrease in noise power; behavior one might reasonably expect. The observed MSE values are from simulation results, averaging the results from 1000 independent realizations of 10,000 QPSK symbols each. The observed MSE behave as predicted by (2.4).

The scenario when there is no interference is the same as an AWGN channel. For a QPSK system the theoretical expression for P_e in the AWGN channel is given by [1]:

$$P_e = Q\left(\sqrt{\frac{2E_b}{N_0}}\right) \tag{2.21}$$

where $Q(x) = \frac{1}{\sqrt{2\pi}}\int_x^{\infty} \exp\left(-\frac{u^2}{2}\right)du$ which calculates the tail probability of a Gaussian distribution.

Figure 2-6 shows P_e, the probability of bit-error performance, for the same system when there is no interference and when ISR = 20 dB and $f_i = 1/e$.

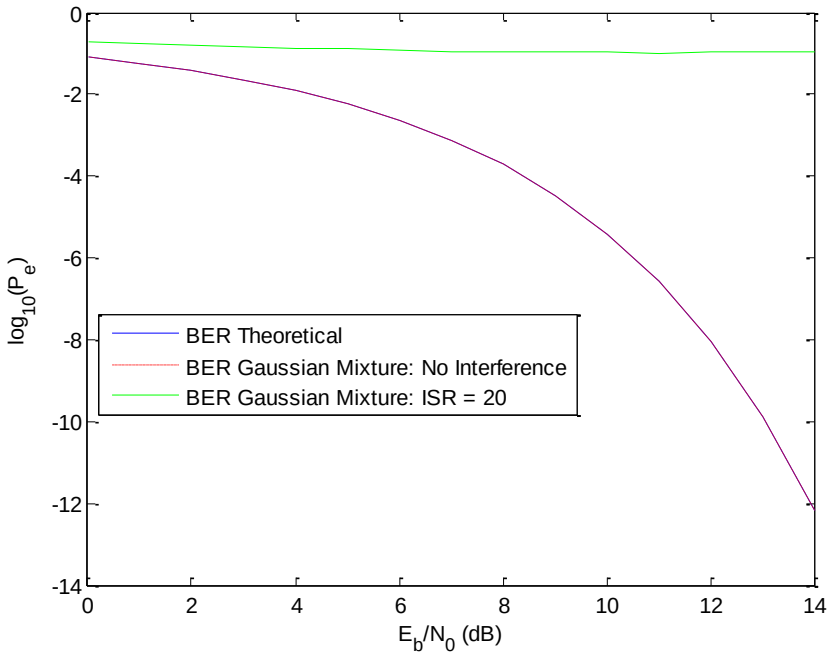

Figure 2-6. P_e performance for L = 3 under no interference and for ISR = 20 dB and f_i =1/e.

As expected, we observe that the curves generated by (2.21) and by the Gaussian Mixture model with ISR = -∞ dB (no interference) in (2.17) are indistinguishable. The curve for ISR = 20 dB shows that performance in terms of probability of bit error has deteriorated substantially when ISR is dominant and – as we already observed from Figure 2-5 – in terms of MSE performance also.

To take a closer look at the case for ISR = 20 dB, we next look at BER performance based on simulation results and its predictions using the GM model described in (2.18) and the Gaussian model described in (2.20).

Figure 2-7 shows the BER performance when there is a strong narrowband interference corrupting the desired signal. For this simulation again ISR = 20 dB, with $f_i = 1/e$ and $f_i = 1/4e$. The observed BER values were generated by Monte-Carlo

simulation, in the same way the observed MSE results were generated for Figure 2-5 earlier.

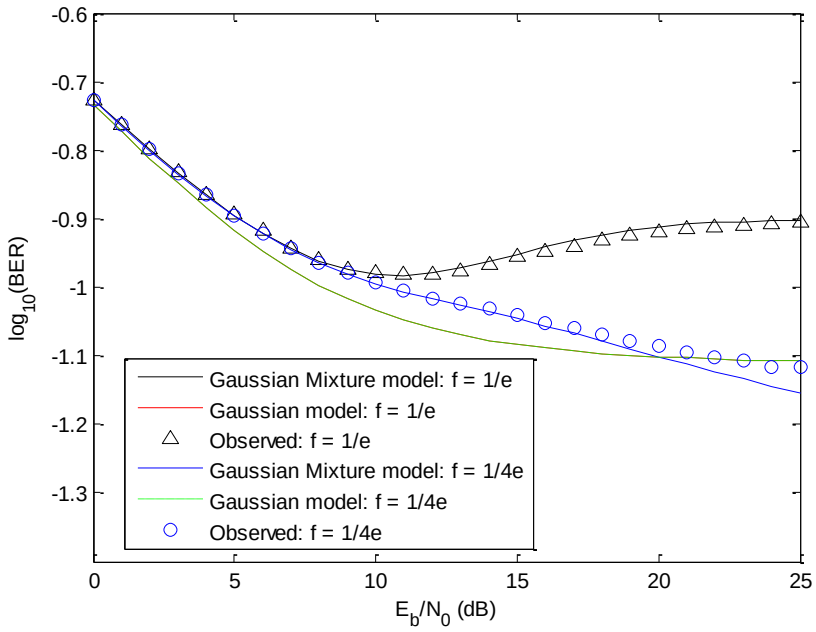

Figure 2-7. BER performance for L = 3 and ISR = 20 dB.

We see that unlike the MSE curve in Figure 2-5 the BER curve is not necessarily monotonically decreasing as noise power is decreasing (or, equivalently, signal power is increasing). This result indicates that MSE and BER are not linked directly, not even in terms of overall behavior. Note that the Gaussian Mixture model from (2.17) provides a good prediction of the BER of the system, for both interference frequencies.

The explanation for the increase in BER when SNR (signal-to-noise ratio) is increasing comes from the Gaussian Mixture model. The centers of gravity (COG) or means for each of the components in the GM model are shown in Figure 2-2 for $f_i = 1/e$. SNR is reflected in the radius of the circular probability mass concentrated at each of these COG. When SNR is low these radii are large and a reduction in these radii corresponds to less probability mass spilling outside of the first quadrant. At some point, after increasing SNR, the radii are small enough that the probability mass associated with the COG inside the first quadrant spills outside less while more of the probability mass

associated with the COG outside of the first quadrant (there are four of these) becomes concentrated outside of the first quadrant. The latter causes the BER to then increase and eventually saturate at the fraction of the number of COG outside the first quadrant relative to the total number of COG. For $L=3$ and $f_i=1/e$ that saturation BER is (4/32=) 0.125 (or -0.9031 dB), while for $L=3$ and $f_i=1/4e$ that saturation BER is (2/32=) 0.0625 (or -1.204 dB). As seen in Figure 2-7, SNR needs to be higher to reach the latter limiting BER, which is understandable from the output constellation in Figure 2-4, since some of the constellation points are very close to a decision boundary (requiring tighter concentration of the probability mass at those COG before the limiting BER is reached).

In Figure 2-7 the performance predicted by the Gaussian model described in (2.20) was shown for the L = 3 case. Figure 2-8 shows the BER performance of the same system under the same strong narrowband interference (ISR = 20 dB), for $f_i=1/e$, but now the equalizer length L is set to 10.

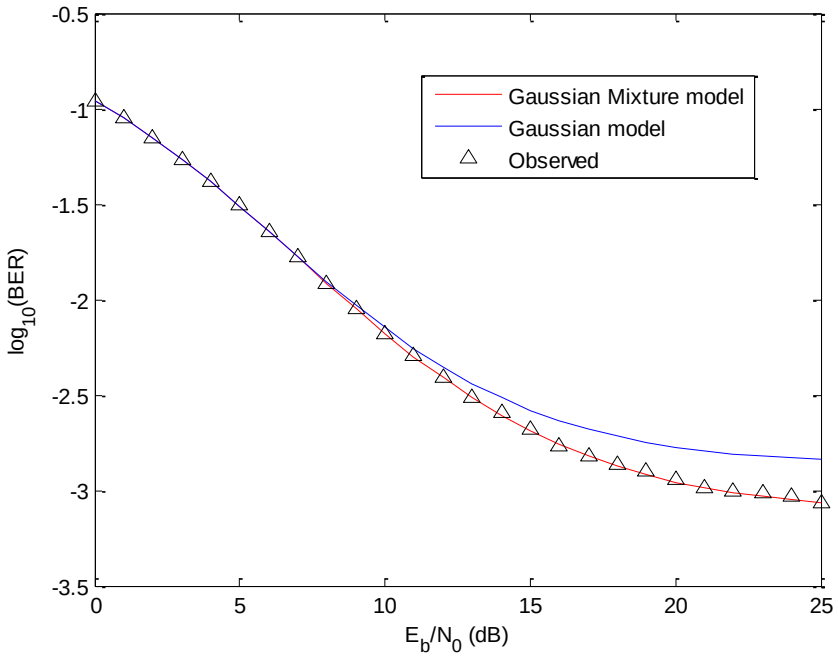

Figure 2-8. BER performance for L = 10 with ISR = 20 dB and f_i =1/e.

While not shown in Figure 2-8, the same experiment was performed also for the different interference frequency $f_i = 1/4e$; the results were completely indistinguishable from those in Figure 2-8.

For L = 3 we saw (in Figure 2-7) that the Gaussian model provided less accurate results than the Gaussian Mixture model, especially at higher SNR. The actual BER performance was over-estimated by the Gaussian model over most of the SNR range. For L = 10 (in Figure 2-8) we see that the prediction of the Gaussian model is now under-estimating actual BER performance but it is much closer to the observed values based on simulation. In fact, for the most practical range of SNR values, E_b/N_0 below 15 dB, the Gaussian model is a reasonably good one for the narrowband interference dominated environment. Observe that the Gaussian sum model provides very accurate results; however, we note that this accuracy comes at the expense of a considerably increased computational burden.

The BER saturation effect is still observed for L = 10, it just happens at a lower level. For larger equalizers the estimation of the narrowband interference gets better, but the residual interference power starts to act as a limiting factor on performance as SNR becomes very large.

For all the above results we have used (2.18) for the GM model and (2.20) for the Gaussian model. Neither of these models considers the effect of the residual interference in the output. This approximation works to a large extent as long as ISR is high. However with a decrease in ISR level, the models in (2.18) and (2.20) tend to deviate from the observed values.

To illustrate this limitation of the GM and Gaussian models described respectively in (2.18) and (2.20) we perform the same simulations as earlier but now with ISR = 5 db. Figure 2-9 shows the result for L = 3 and $f_i = 1/e$.

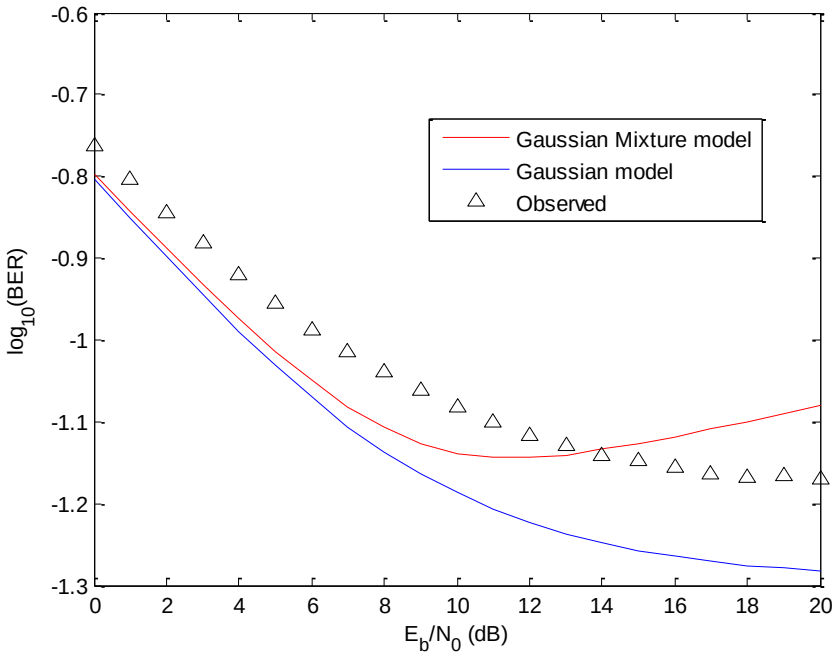

Figure 2-9. BER performance for L = 3 with ISR = 5 dB and f_i =1/e.

For a lower ISR level both models overestimate the system performance. When the ISR level is low, the residual interference present in the output is comparable to the other two components. As these models neglect that component, the system performance is overestimated.

It is not surprising to find that with a decrease in ISR the residual interference component in the output actually increases. This stems from the fact that the Wiener filter operates on the principle of minimizing MSE. High level ISR corresponds to an interference signal which is considerably more dominant than the AWGN. So the Wiener filter tries to minimize that effect and in turn cancels the interference efficiently. However, when the ISR level is comparable to the noise power, the Wiener filter tries to mitigate the effects of both noise and interference. This trade-off causes the presence of an interference component in the output.

The GM and Gaussian models described respectively in (2.17) and (2.19) take the interference component into account and hence are more robust. Figure 2-10 shows their

performance. Simulation Environment identical to the one used to generate Figure 2-7 was used in this case, only difference being ISR was set to 5 dB instead of 20 dB.

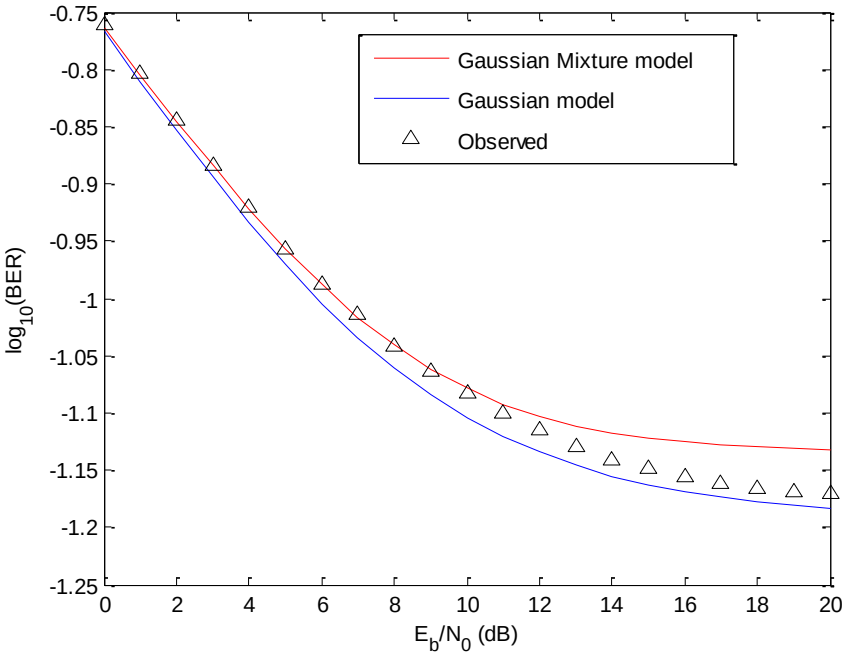

Figure 2-10. BER performance for L = 3 with ISR = 5 dB and f_i =1/e with the improved model.

From Figure 2-10 it is clear that the GM and Gaussian models described in (2.17) and (2.19) respectively provide pretty accurate results. A similar experiment was conducted with the GM and Gaussian models and an ISR = 20 dB. The results were indistinguishable from Figure 2-7. Another observation is that the models work better for the lower E_b/N_0 values (< 12 dB) than for the higher ones. This is a direct result of the assumption that we made in Section 2.2.3 regarding the PDF of y_n^i. The PDF of y_n^i, originally an Arc-sine distribution, was approximated with a Gaussian. A random variable following an Arc-sine distribution only takes values from a finite interval with non-zero probability whereas a Gaussian random variable can assume any complex value. So, as we are replacing a bounded distribution by an unbounded one, the area enclosed by the curve increases and the GM model underestimates the system performance. For the lower E_b/N_0 region the presence of a dominant AWGN in the output imparts a

sufficiently Gaussian characteristic and hence the BER predicted by the Gaussian model is quite close to the observed value.

2.6 Summary

We have shown that the BER performance of a Wiener equalizer based digital communication system – when operating in a narrowband interference dominated environment – does not always follow along with the MSE performance. The BER performance of the system can be predicted accurately using the Gaussian sum model that was proposed. For practical considerations where larger equalizer filters are used, the Gaussian Mixture model can be approximated using a Gaussian model which is then much more efficient computationally.

CHAPTER 3 BER MODELING FOR ADAPTIVE (N)LMS EQUALIZER USING STEADY STATE WEIGHTS

In the previous chapter we discussed at length BER models that can be used to predict the BER of a communications system which uses a Wiener Equalizer. In order to find the optimum Wiener Weights we need to know the signal statistics of all the signals involved. This information may not be available in a practical situation. For this reason adaptive equalizers are often used instead of the Wiener equalizer. In this chapter, we investigate the BER performance of the Least Mean Square (LMS) class of adaptive equalizers for an environment which is dominated by narrowband interference.

The chapter begins by motivating the topic where simulation results are used to highlight the superior performance of an adaptive equalizer over its Wiener counterpart. Then we take a detour and define some terms related to LMS equalizers. A model is proposed that describes the BER performance of the adaptive equalizer followed by simulation results. The results are then analyzed highlighting the contrast between the two cases – the Wiener and the adaptive equalizers.

3.1 Motivation

The FIR Wiener Filter is considered to be the optimal solution given that we know the signal statistics of all the signals involved. The primary argument behind opting for adaptive filters is their ease of implementation since they do not need any prior knowledge of the signals involved. So even at the cost of sub-optimal performance practical systems often prefer an adaptive equalizer over the optimal Wiener one.

In an environment dominated by narrowband interference, non-Wiener effects are observed when using LMS equalizers. Figure – 3.1 shows the comparison between an adaptive (N)LMS equalizer and a fixed FIR Wiener equalizer in terms of Mean Square Error (MSE) as a function of the normalized step size (μ). We simulated an environment

which had a Gaussian white noise (SNR = 25 dB) and a narrowband interference simulated by a tone having a fractional frequency of $f_i = 1/e$ with ISR = 20 dB. For both of these cases, the length of the equalizer was set to $L = 5$.

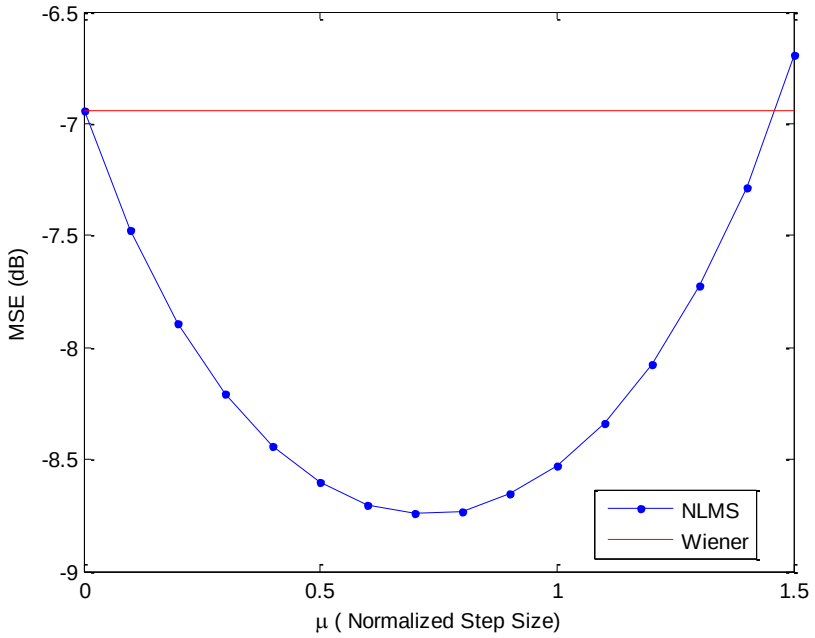

Figure 3-1. Comparison between NLMS and Wiener Equalizers in terms of Mean Square Error (MSE).

From Figure 3-1, we see that the adaptive NLMS equalizer outperforms the optimal Wiener filter in terms of MSE by approximately 2 dB. However, for practical communication systems Bit Error Rate (BER) is a preferred metric of performance over MSE. Figure 3-2 compares BER performance of the two systems as a function of μ. The simulation environment was identical to the one that was used to generate Figure 3-1.

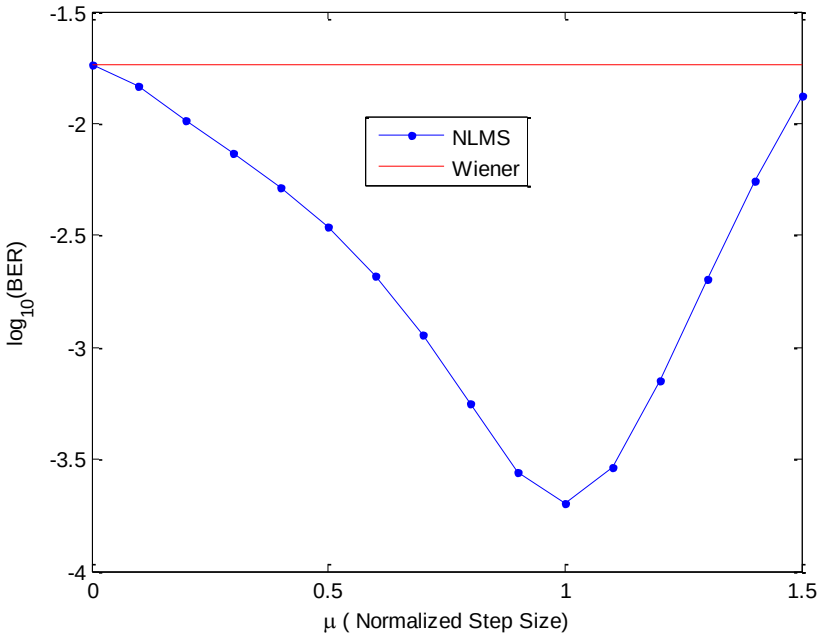

Figure 3-2. Comparison between NLMS Equalizer and Wiener Equalizer in terms of Bit Error Rate (BER).

From Figure 3-2 we see that a 2 dB improvement in the MSE results in an improvement of 2 orders of magnitude in BER. These simulation results point out that the (N)LMS class of equalizers is not only simpler to implement, they are also performing substantially better than their Wiener counterpart – both in terms of MSE and BER.

There are a couple of interesting observations from Figures 3-1 and 3-2. Conventionally, adaptive equalizers are operated with low step sizes (typically $\mu < 0.1$). We observe here that the adaptive equalizer performs optimally both in terms of MSE and BER for large step sizes ($\mu > 0.7$). We also notice that the optimal performance in terms of MSE and BER occurs at different step-sizes. The adaptive equalizer delivers the optimal performance in terms of MSE for $\mu \approx 0.7$, whereas the optimal performance in terms of BER is observed for $\mu \approx 1$. This is similar to what we observed in the previous chapter, in that MSE and BER were not following the same trend.

So we see that the adaptive equalizer outperforms the Wiener equalizer in terms of BER and MSE. The main aim of this work is to find a mathematical model which will accurately describe the BER performance of the adaptive equalizer.

3.2 Adaptive (N)LMS Equalizers: Update Equations & Steady State Weights

Figure 3-3 shows a block diagram of an adaptive equalizer.

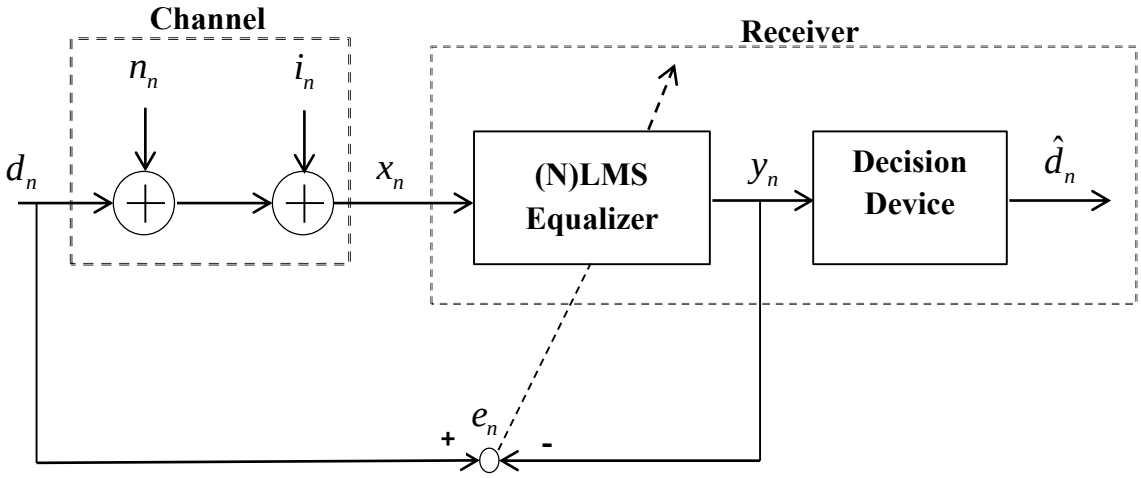

Figure 3-3. Block Diagram of an Adaptive Equalizer.

All the input signals shown in this block diagram are identical to the ones that were depicted in the block diagram for the Wiener Case in Figure 2-1. The only difference is the error signal at the *n*-th instant denoted by e_n and defined as follows:

$$e_n = d_n - y_n \tag{3.1}$$

3.2.1 Update Equation

The error feedback is utilized to update the filter weights at each instant. The update equation for the Normalized Least Mean Square (NLMS) is given by [11]:

$$\mathbf{w_{n+1}} = \mathbf{w_n} + \frac{\mu}{a + \|\mathbf{x_n}\|^2} \mathbf{x_n} e_n^* \tag{3.2}$$

where $\mathbf{w_n}$ is the filter weight vector at the *n*-th instant and a is the regularization parameter. The regularization parameter is present to ensure that we do not run into a division by a very small number – a situation which may arise if the input energy of the tapped delay line is (temporarily) small, i.e. $\|\mathbf{x_n}\|^2 \approx 0$.

3.2.2 Steady State Weights

For most applications, the LMS algorithm converges to match the performance of the corresponding optimal Wiener Filter. The steady state weights of the adaptive filters also converge to the corresponding Wiener weights. In the case of an environment dominated by a narrowband interference however, we see the non-Wiener characteristics of LMS equalizers and the steady state (N)LMS weights have been shown not to converge to the corresponding Wiener weights.

A closed form expression of the steady state NLMS weights is given below [19, 21]:

$$\mathbf{w_{ss}} = \eta(\mathbf{p}_\Delta - \tilde{\mathbf{w}}) \tag{3.3}$$

where,

$$\eta = \frac{\sigma_\phi^2}{\sigma_\phi^2 + \sigma_n^2}$$
$$\mathbf{p_\Delta} = \begin{bmatrix} 0 & \dots & 0 & 1 & 0 & \dots & 0 \end{bmatrix}^T \tag{3.4}$$

The vector $\mathbf{p}_\Delta$ is of length L and has Δ zeros before 1. As explained in Chapter 2, Δ is the center of equalization. Following the same notation as in Chapter 2, σ_ϕ^2 and σ_n^2 respectively denote the signal power and the noise power.

The remaining term in (3.3), $\tilde{\mathbf{w}}$ is defined as –

$$\tilde{\mathbf{w}} = (\mathbf{I} - \frac{\mu}{L(\sigma_n^2 + \sigma_i^2)} \mathbf{R_x}^{-1}\mathbf{Q})^{-1}\mathbf{w}_w \tag{3.5}$$

where $\mathbf{I}$ is the identity matrix of size $L \times L$, $\mathbf{R_x} = E\left\{\mathbf{x}_n \mathbf{x}_n^H\right\}$, σ_i^2 is the interference power, and $\mathbf{Q}$ is given by:

$$\mathbf{Q} = \sigma_n^2 \sigma_i^2 L \sum_{k=1}^{L-1} \mathbf{Z}^k e^{-j\omega_i k} \gamma^{k-1} \tag{3.6}$$

where $\mathbf{Z}$ is a unit lower triangular Toeplitz matrix where all the non-zero elements are set to 1, $\gamma = 1 - \mu\lambda_{\max}$, $\lambda_{\max} = L\sigma_i^2 + \sigma_n^2 + \sigma_\phi^2$, and $\mathbf{w_w}$ is the corresponding Wiener weight vector.

It is clear from (3.3) and (3.5) that if $\mu = 0$ the steady state NLMS weight vector $\mathbf{w_{ss}}$ is the same as the Wiener weight vector $\mathbf{w_w}$. This result is consistent with our intuition since $\mu = 0$ implies a fixed filter and for that case the Wiener filter is indeed the optimal solution.

3.3 Gaussian Mixture using Steady State Weights Model

With the basic definitions and notations in place, we try to find a model that will accurately determine the BER performance of a digital communications system that has an adaptive LMS equalizer. As an initial model we propose a Gaussian Sum Model (GSM) similar to the one proposed in (2.17). The only difference between the two cases is the fact that instead of using the Wiener weights we use the steady state NLMS weights.

The conditional PDF $f\left(y_n \middle| d_{n-\Delta} = \phi_m\right)$ for an interference dominated environment is expressed by:

$$f\left(y_n \middle| d_{n-\Delta} = \phi_m\right) \cong \frac{1}{M^{L-1}} \sum_{k_1,\cdots,k_{L-1}=1}^{M} CN\left(\mu_{m\mathbf{k}}, \left\|\mathbf{w}_{\mathbf{ss}}\right\|_2^2 \sigma_n^2\right)$$
$$\mu_{m\mathbf{k}} = w_j^{ss^*} \phi_m - \sum_{\substack{l=1 \\ l \neq j}}^{L-1} w_l^{ss^*} \phi_{k_i} \tag{3.7}$$

The deduction is exactly similar to the one shown in Section 2.2. This model is termed the Gaussian Mixture using Steady State Weights (GMSSW) model to differentiate it from the GM model introduced in Section 2.2.

From (3.7), we find the BER estimate for the system by evaluating the volume enclosed by the complex normal distribution in the regions corresponding to a bit error. The regions are determined by the appropriate decision rules.

3.4 Simulation Results

For simulation purposes, we use a digital communication symbol which uses a QPSK modulation scheme, i.e. d_n are QPSK symbols, which implies $M = 4$. The narrowband interference signal is represented by a complex sinusoid, as in (2.12).

With this environment, we proceed to compare the performance of our model with the simulated results. The simulated results were generated taking the ensemble average of 100 independent realizations with 100,000 independent symbols generated for each realization. Figure 3-4 shows a comparison of the simulated BER with the theoretical BER calculated by (3.7) as a function of μ . The equalizer length L is taken to be 3 with SNR = 25 dB, ISR = 20 dB, and $f_i = 1/e$.

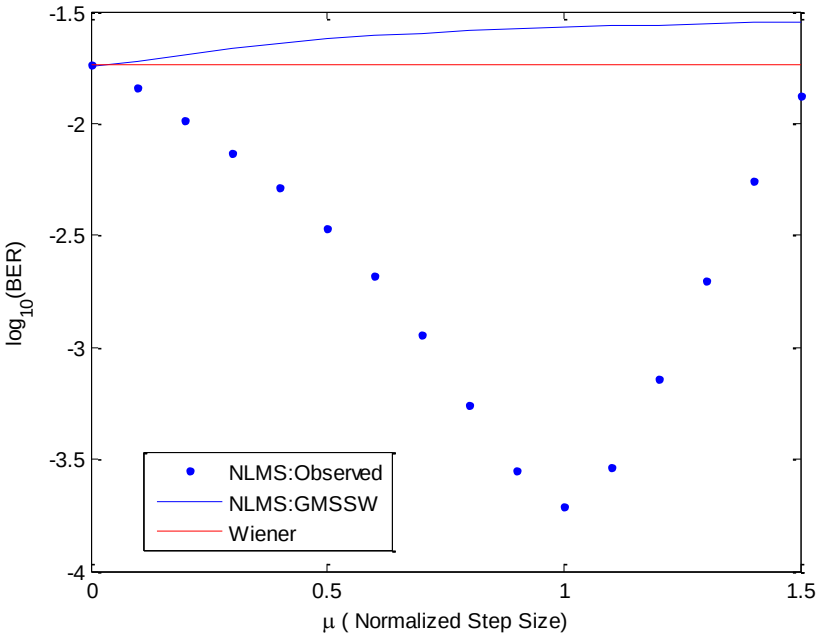

Figure 3-4. Comparison between observed and theoretical GMSSW model BER for L = 5 as a function of μ.

From Figure 3-4 we see that the model is unable to capture the BER performance of the system. The model in fact produces a different trend, i.e. it is monotonically increasing with an increase in step size whereas the observed values show a decrease in BER for $0 < \mu < 1$, with a subsequent increase.

Figure 3-5 shows the comparison of observed and theoretical BER (GMSSW model) as a function of SNR. A step size of $\mu = 1$ is chosen and all the other parameters are kept the same as before.

We clearly see that the GMSSW model is unable to track the BER for a varying SNR. The model in this case predicts a decreasing trend but the rate of decrease is much slower than what is actually observed.

Although the model is inaccurate, it is worthwhile to investigate why the model did not work in spite of the fact that it worked very well in the case of a fixed Wiener equalizer, as shown in Figures 2-7 and 2-8. In the next section we will analyze the results

thoroughly in order to come up with an explanation for the reasons underlying the failure of the GM model in the adaptive case.

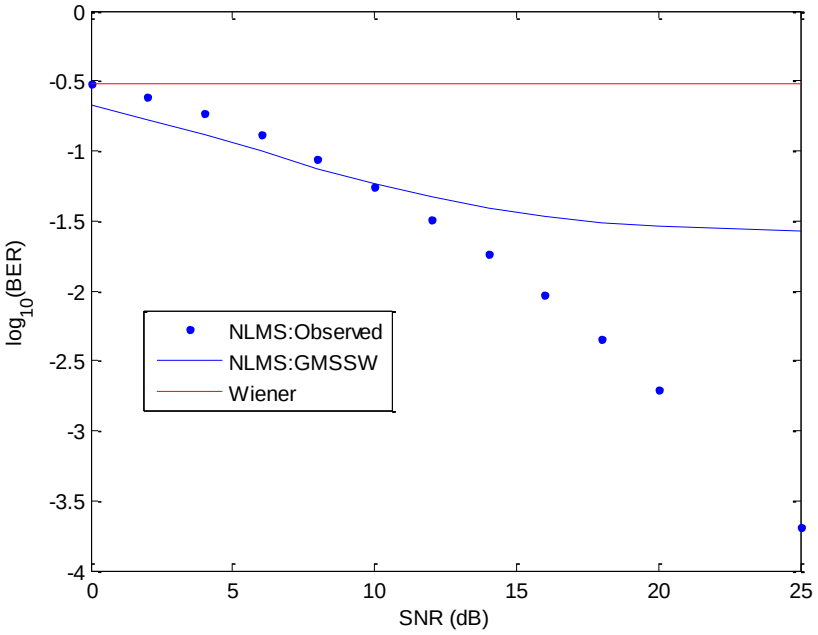

Figure 3-5. Comparison between observed and theoretical GMSSW BER for L = 5 as a function of SNR.

3.5 Discussions

The output y_n of the equalizer at any instant can be thought of as a result of summing three components – the desired signal component y_n^d, the noise component y_n^n and the interference component y_n^i. We can then write:

$$\begin{aligned} y_n &= \mathbf{w_n^H x}_n \\ &= \mathbf{w_n^H d}_n + \mathbf{w_n^H i}_n + \mathbf{w_n^H n}_n \\ &= y_n^d + y_n^i + y_n^n \end{aligned} \tag{3.8}$$

It is to be noted here that this equation looks similar to (2.2). However, the systems in the two cases are entirely different. A fixed Wiener filter is an LTI system,

while the adaptive filter is a time varying system. However, even for the time varying filter at each instant the output can be thought of as being a summation of these three components. The idea is similar to the one that we adopted while deriving GM model in Section 2.2. We will investigate each component separately and try to gauge how they are interacting.

For illustrative purposes, we take the equalizer length $L = 3$. For a QPSK system with $M = 4$, the number of conditional output constellation points should be $M^{L-1} = 16$. A higher value of L will result in an enormous number of constellation points and it will be difficult to visualize.

Figures 3-6 (a-d) shows the conditional output constellation map $y_n^d \mid d_{n-\Delta} = \phi_m$ for four different step sizes $(\mu = 0, 0.1, 0.5, 1)$. We generated 10,000 independent QPSK symbols with SNR = 25 dB, ISR = 20 dB, and $f_i = 1/e$. For this figure we are conditioning on the symbol of the QPSK modulation scheme that occurs in the first quadrant.

Figure 3-6 points out a few interesting things. Figure 3-6 (a) is the Wiener case and it is identical to Figure 2-2, which is as expected. This also provides us with a sanity check that if the normalized step size $\mu = 0$ the steady state NLMS weights indeed converge to the Wiener weights. Figure 3-6 (b) shows sixteen blobs roughly centered around the output constellation points shown in Figure 3-6 (a). This is also expected since the blobs signify that there are minor deviations from the steady state values.

Figure 3-6 (c) shows that there are twelve blobs. Although this looks like a deviation from the number of output constellation points predicted by the GMSSW model, actually we can see from the Figure 3-6 (c) there are four instances where a pair of blobs converged to become a single one. Figure 3-6 (d) further corroborates this point.

From Figure 3-6 we can conclude that at higher step sizes non-Wiener effects play a dominating part. The output constellation map is similar to the one predicted by

GMSSW model although for higher step sizes two blobs can merge to form a single one. It also shows that the step size μ has a significant effect on the output constellation map.

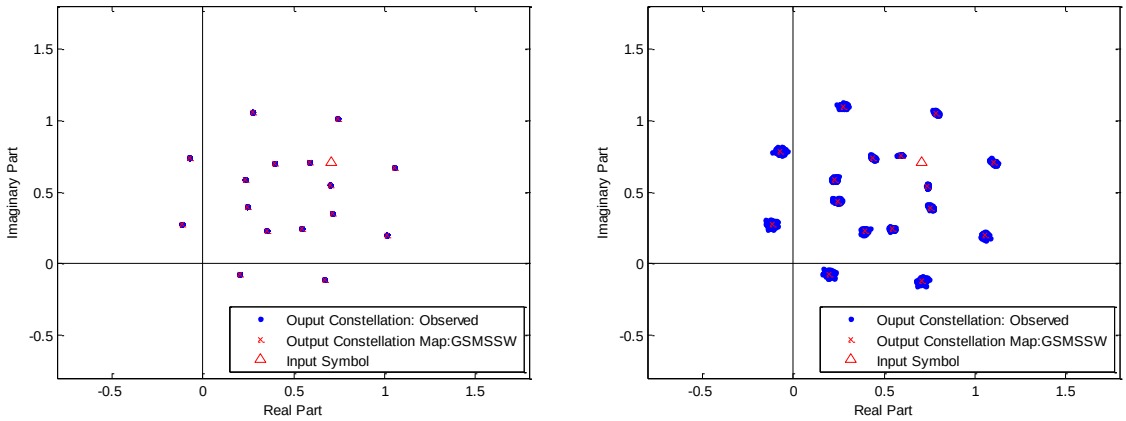

(a) μ = 0 (Wiener Filter) **(b) μ = 0.1**

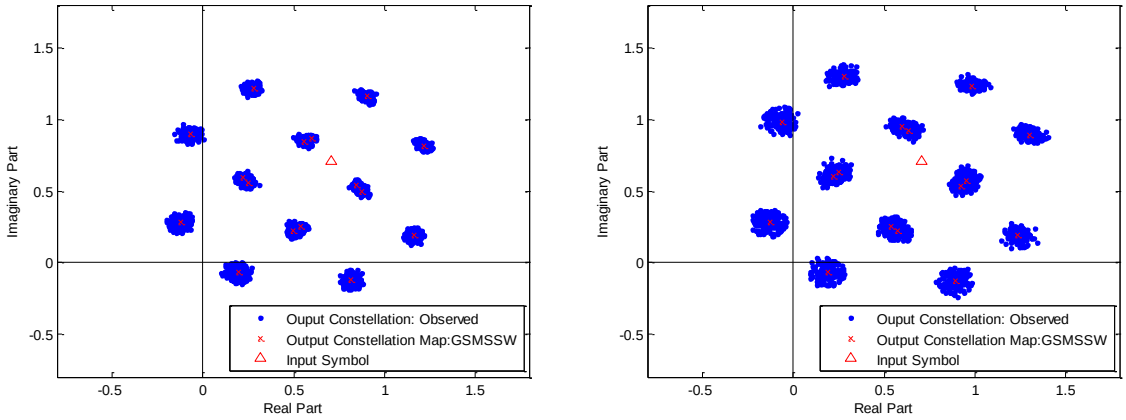

(c) μ = 0.5 **(d) μ = 1**

Figure 3-6. Conditional output constellation map for L = 3 for four different step sizes.

Figures 3-7 (a-d) shows the noise component for the same step sizes as in Figure 3-6. We notice that the noise component is independent of the step size. This indicates the conditional PDF for the noise component, i.e. $f(y_n^n \mid d_{n-\Delta} = \phi_m)$ is the same as the one described in (2.7) with the Wiener weights $\mathbf{w}$ replaced by the steady state NLMS weights $\mathbf{w}_{ss}$.

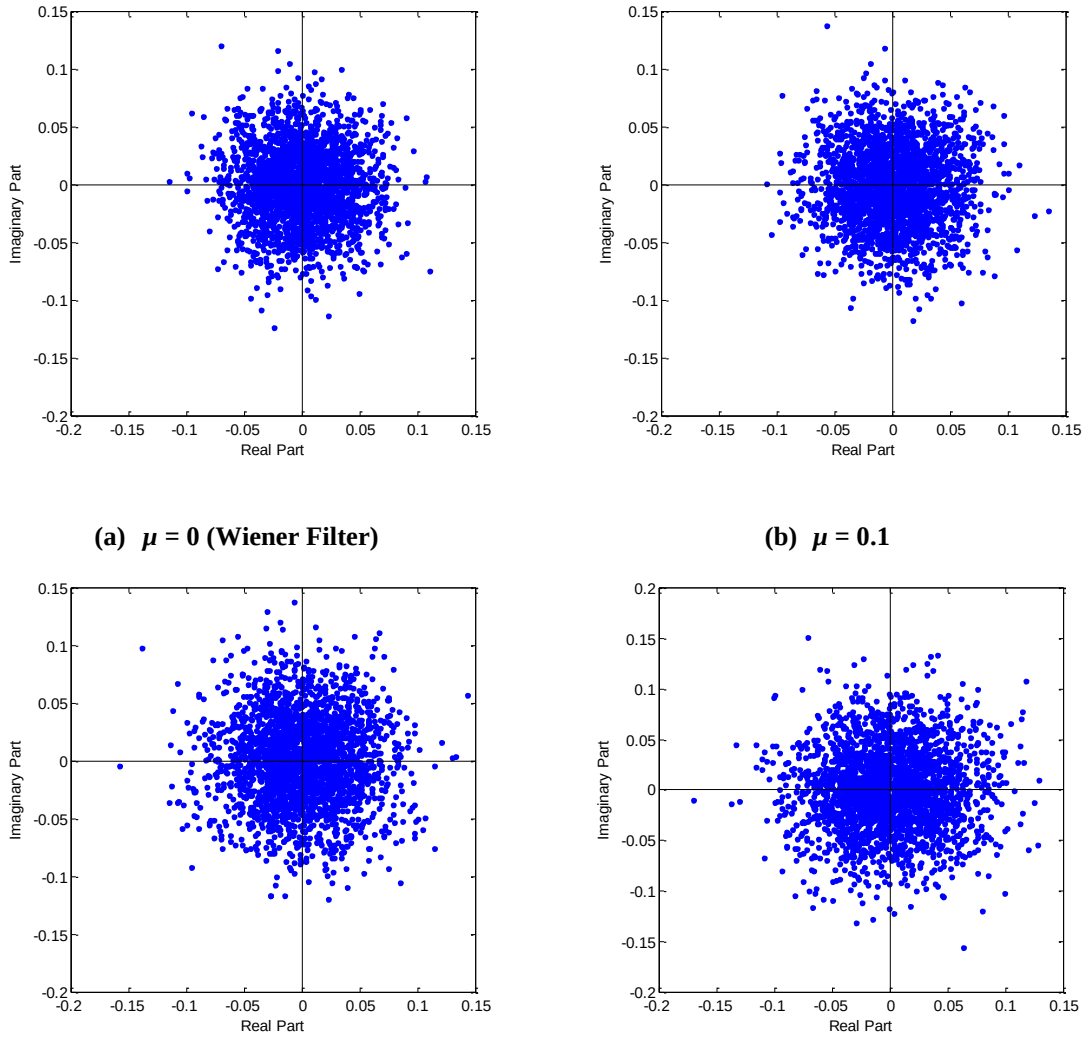

(a) μ = 0 (Wiener Filter) **(b) μ = 0.1**

(c) μ = 0.5 **(d) μ = 1**

Figure 3-7. Conditional output noise component for L = 3 for four different step sizes.

Figures 3-8 (a-d) shows the conditional output interference component for the same setup. Figure 3-8 (a) shows the Wiener filter case where the output is a complex sinusoid. This result is consistent with the fact that the Wiener filter is a LTI system and a complex sinusoid in the input will produce a scaled and shifted version at the output. It is to be noted that the magnitude of the sinusoid at the output is extremely small, compared to the input sinusoidal power, 20 dB in this case, which implies that the Wiener filter is successfully suppressing the interference.

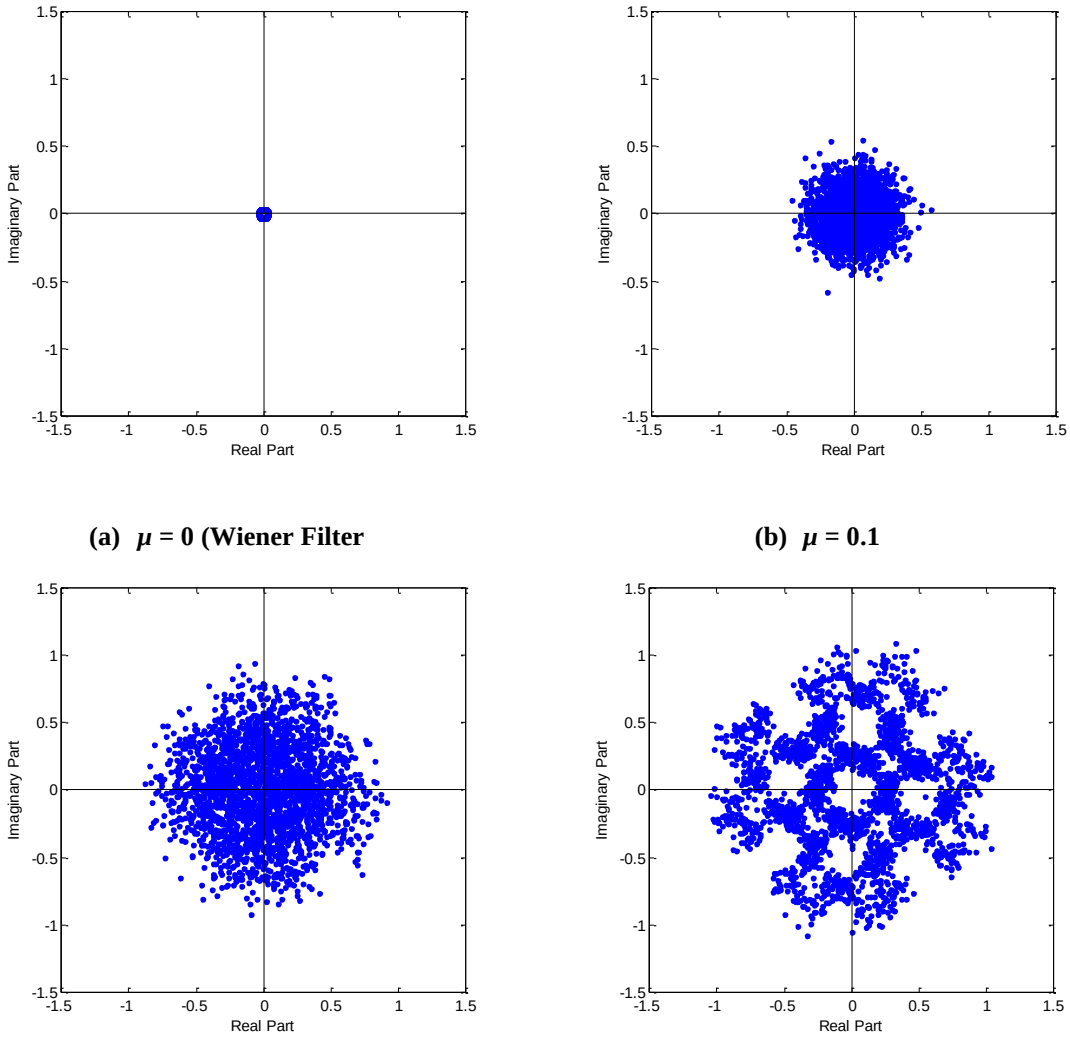

(a) μ = 0 (Wiener Filter

(b) μ = 0.1

(c) μ = 0.5

(d) μ = 1

Figure 3-8. Conditional output interference component for *L* = 3 for four different step sizes.

Figure 3-8 (b) shows the output interference component when the step size $\mu = 0.1$. By comparing Figure 3-8 (b) with Figure 3-8 (a) we clearly see that the output conditional PDF is different in each case. We also note that the variance of the interference component in Figure 3-8 (b) is now substantially higher than in Figure 3-8 (a).

Figures 3-8 (c) and 3-8 (d) further provide us with the contrast in the output interference component compared to Figure 3-8 (a). We notice similar trends – the output

is not a complex sinusoid as was the case with the Wiener filter and the variance is substantially higher. We can conclude that the interference component is also significantly different in the case of an adaptive filter than what it was with a fixed filter.

GM model neglects the interference component at the output. That assumption worked well in the fixed case since, for high ISR cases, the interference component is practically negligible. However, we can clearly see from Figures 3-8 (b-d) that the interference component for the adaptive case is not at all negligible. The variance as seen in Figures 3-8 (c-d) is relatively high considering that $\sigma_{\phi}^{2} = 1$. This points to a shortcoming of the GMSSW model.

Figures 3-9 (a-d) show the conditional output $y_n \mid d_{n-\Delta} = \phi_m$. Figure 3-9 (a) shows the output corresponding to the Wiener filter. Once again this is consistent with the results that we have seen in Chapter 2. The Gaussian Mixture model was successful in describing this since the output was simply a summation of sixteen Gaussian variables centered at different output constellation mapping points shown in Figure 3-6 (a). The variance of each of those Gaussian distributions is the same as the variance of the noise shown in Figure 3-7 (a).

Figure 3-9 (b) shows the conditional output for a step size $\mu = 0.1$. We cannot isolate the centers as we were able to do in Figure 3-9 (a). In Figures 3-9 (c) and (d) we observe similar trends where we are not able to discern individual centers. The assumption that worked in favor of GMSSW model for Figure 3-9 (a) no longer hold true for Figures 3-9 (b-d). The output components are no longer independent of each other which implies that the conditional PDF $y_n \mid d_{n-\Delta} = \phi_m$ does not result from the convolution of the three constituent PDFs, to wit $f(y_n^n \mid d_{n-\Delta} = \phi_m)$, $f(y_n^d \mid d_{n-\Delta} = \phi_m)$ and $f(y_n^i \mid d_{n-\Delta} = \phi_m)$. As a result, the GMSSW model is unable to capture the non-Wiener effects for higher step sizes. The interaction between the output components is discussed in the remainder of this chapter.

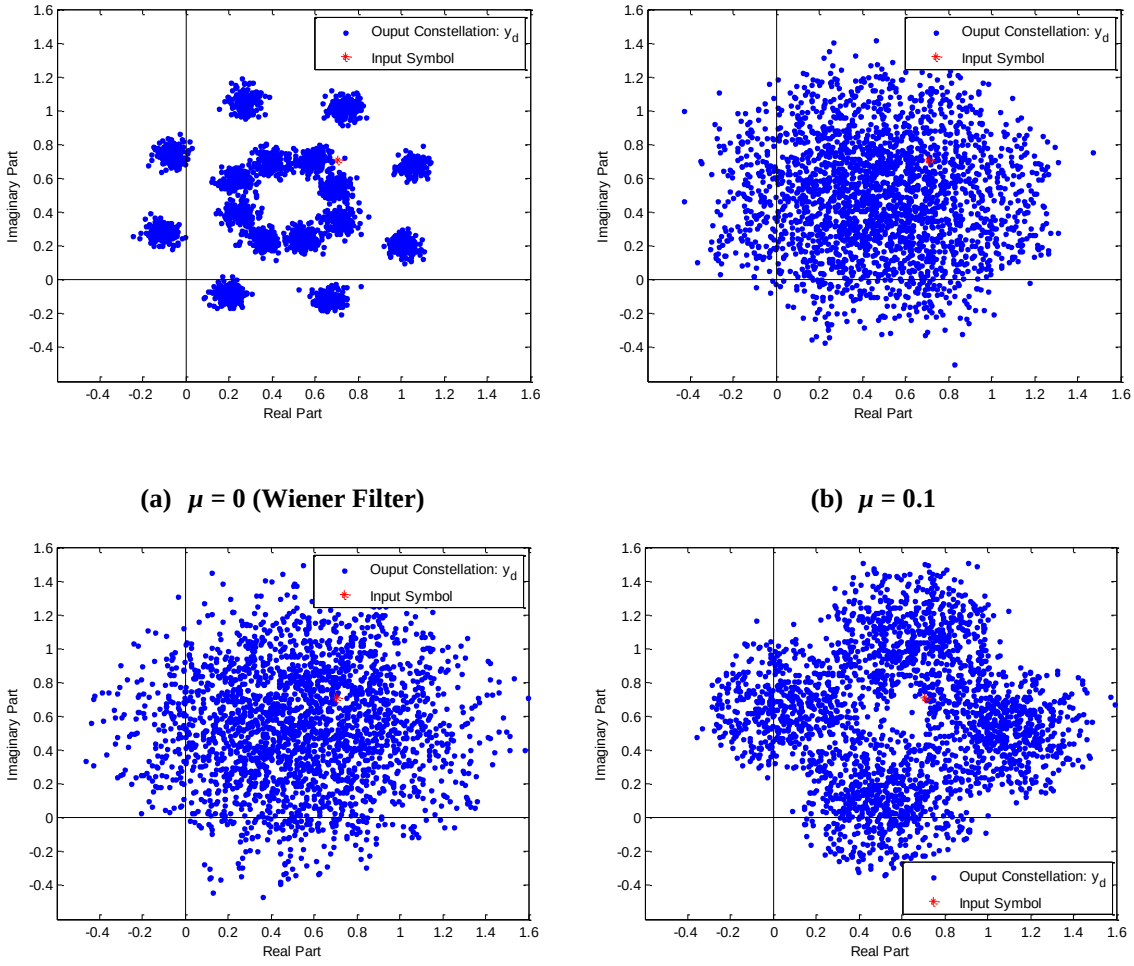

(a) μ = 0 (Wiener Filter) **(b) μ = 0.1**

(c) μ = 0.5 **(d) μ = 1**

Figure 3-9. Conditional output component for L = 3 for four different step sizes.

From the simulation results in Figure 3.4 we observed that the BER was decreasing with an increase in step-size within a certain range $(0 < \mu < 1)$. From Figures 3-9 (b-d) we observed that the variance of the interference component is increasing as we increase the step size from 0 to 0.1 and then to 0.5 and finally to 1. These two phenomena seem counter intuitive as a higher variance of the interference component indicates that the interference was not successfully mitigated and hence should result in a poorer BER performance. However, we observe the opposite, i.e. an increase in the variance of the interference component results in the decrease of BER.

We now investigate this case in detail. Figure 3-10 shows the conditional output constellation (for an equalizer of length $L=5$) with the three colored points denoting three points which are in the wrong quadrant (since we are conditioning on the first quadrant symbol). The step size was set to $\mu=1$, with SNR = 25 dB, ISR = 20 dB, and $f_i=1/e$.

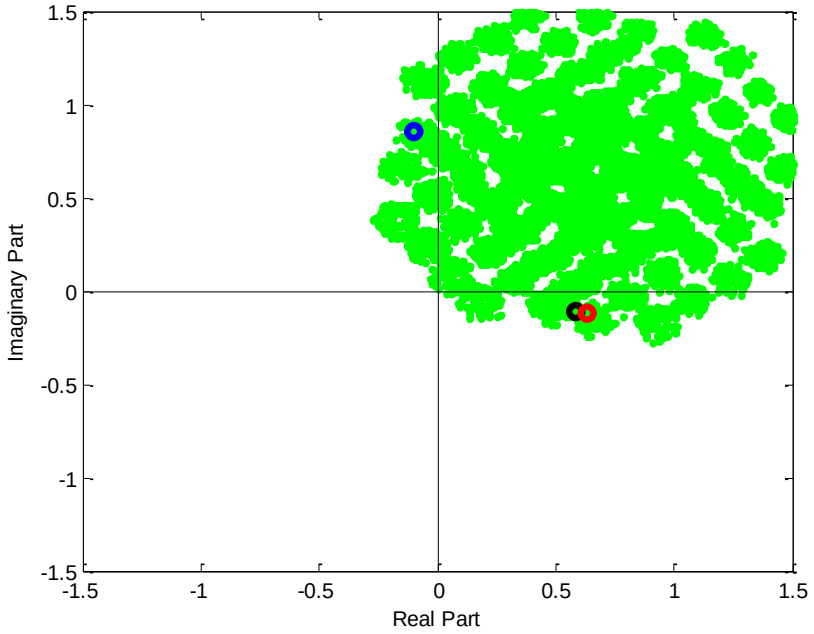

Figure 3-10. Conditional output constellation highlighting three error points.

Figure 3-11 shows the corresponding conditional interference component. The three colored points correspond to the points which were in the wrong quadrant in Figure 3-10. We notice an interesting trend by observing Figures 3-10 and 3-11. If we consider the blue point in Figure 3-10 we see that the point is in the second quadrant. In order to shift it to the correct quadrant we need to add a term which has a positive real part. The corresponding interference component in Figure 3-11 has a positive real part and thus it pushes the blue point in Figure 3-10 into the correct quadrant. Similarly the black and the red points needed a term with a positive imaginary part. The corresponding interference component provides exactly that and shifts them into the correct quadrant.

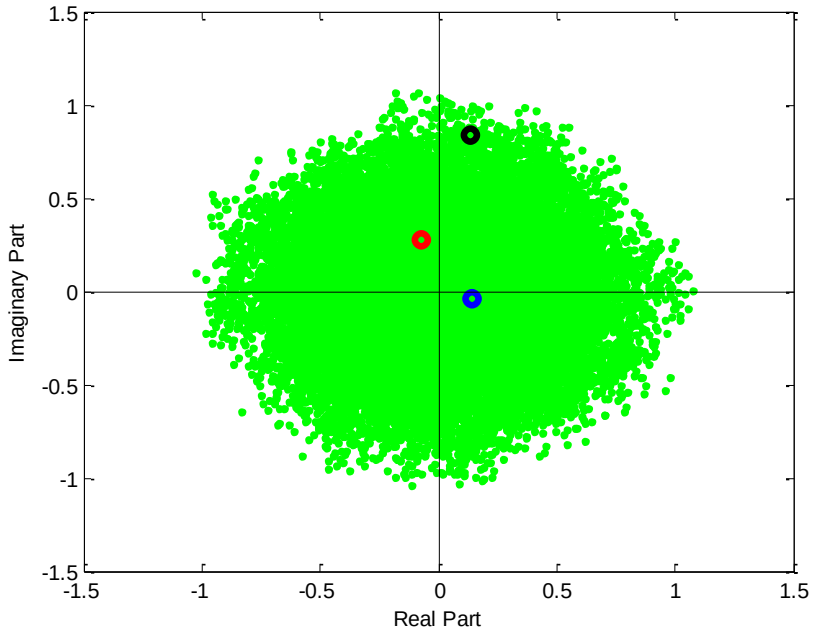

Figure 3-11. Conditional interference component highlighting the points corresponding to the three wrong quadrant points shown in Figure 3-10.

Figure 3-12 shows the conditional output highlighting the same three points as shown in Figures 3-10 and 3-11. We observe that those points which were in the wrong quadrant, as shown in Figure 3-10, have been shifted into the correct quadrant. Figure 3-12 shows that there are points which are in the wrong quadrant and thus will be treated as an error. However, this number turns out to be significantly less than the number of points in incorrect quadrants in Figure 3-10.

For example, in this simulation there is a total of 25044 first quadrant symbols, which means that in each of Figures 3-10 to 3-12 we have 25044 green points. Among those 25044 points in Figure 3-10 there are 1390 points which are in wrong quadrants. However, from Figure 3-12 we observe that the number of points in the wrong quadrant has been reduced to 6 which gives a bit error rate of $\frac{6}{25044} = 2.4\times10^{-4} = 10^{-3.62}$. Note that the bit error rate observed for a step size of $\mu = 1$ is $1.9\times10^{-4} = 10^{-3.72}$ as shown in Figure 3-4. These two results are statistically consistent. Figures 3-10 to 3-12 indicate that the adaptive (N)LMS equalizer exploits the narrowband interference to its advantage

and outperforms the corresponding Wiener equalizer which only tries to mitigate the interference in a Mean Square Error sense.

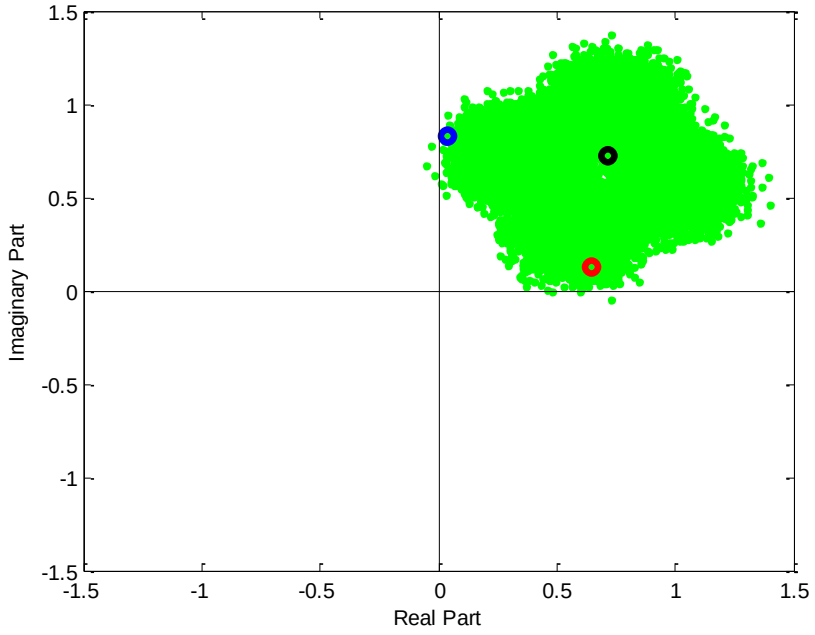

Figure 3-12. Conditional output highlighting the points corresponding to the three wrong quadrant points shown in Figure 3.10.

3.6 Summary

In this chapter, we introduced a BER model – termed GMSSW – which was similar to the one that we used for the fixed Wiener filter. Although the GM model worked well for the Wiener filter, simulation results showed that GM model was not accurate for the adaptive NLMS case. We investigated the reasons for its failure and highlighted the differences between the Wiener and the adaptive case. We also put forth a plausible explanation behind the superior BER performance of the NLMS equalizer over the Wiener equalizer.

CHAPTER 4 BER MODELING FOR ADAPTIVE (N)LMS EQUALIZER USING MEAN SQUARE ERROR

In the previous chapter we introduced a BER model which uses the steady state weights for the (N)LMS equalizer and termed it the GMSSW model. We observed that the model was inadequate as it failed to capture the non-Wiener characteristics of the (N)LMS equalizer. In this chapter we propose a different model towards more accurate estimation of BER.

The chapter is organized as follows. We start by stating the expression for the steady state error for a (N)LMS equalizer in an environment dominated by a narrowband interference followed by our proposed model. The performance of the model is compared to observed values as well as with our previous GMSSW model in the next section and the results is analyzed in the final section.

4.1 Steady State Mean Square Error for (N)LMS Equalizer

For the Wiener equalizer, the closed form expression of MSE is well known (2.4). In fact, the MSE for the Wiener equalizer is termed the minimum MSE (MMSE) since it was the optimal solution. From Figure 3-1, we can clearly see that the NLMS equalizer outperforms the Wiener equalizer in terms of MSE. As explained in Section 3.2.2, for a narrowband interference dominated environment the steady state NLMS weights do not converge to the Wiener solution.

However, in an environment dominated by narrowband interference the MSE performance is better than for the Wiener filter, i.e. MSE can converge to less than the corresponding MSE for the Wiener filter. The closed form expression for the steady state MSE for a narrowband interference cancelling NLMS equalizer is given in [22]

$$J = \frac{2\eta}{1+\alpha}\left[\sigma_n^2 + \sigma_x^2\left\{\left\|\mathbf{w_{ss}}\right\|^2 - (1-\alpha)\left|\mathbf{w_{ss}}\right|^T \mathbf{A}\left|\mathbf{w_{ss}}\right|\right\}\right] \tag{4.1}$$

where

$$\alpha = 1 - \mu\frac{\sigma_i^2 L}{\sigma_i^2 + \sigma_n^2 + \sigma_d^2} \tag{4.2}$$

$$\mathbf{A} = \begin{bmatrix} 0 & & \cdots & & 0 \\ 1 & 0 & & & \\ \alpha & 1 & \ddots & & \vdots \\ \vdots & & \ddots & 0 & \\ \alpha^{L-2} & & & 1 & 0 \end{bmatrix}$$

The MSE expression given in (4.1) models the non-Wiener characteristics of the NLMS equalizer. In the following section we introduce a model which uses this MSE to describe the BER behavior of the NLMS equalizer.

4.2 Gaussian using Mean Square Error Model

The conditional PDF of interest given by $f\left(y_n \left| d_{n-\Delta} = \phi_m \right.\right)$ fixes the equalization point in $\mathbf{x}_n$ which is multiplied by the corresponding element in the weight vector w_n^{Δ}. We can write the summation as follows:

$$\begin{aligned} y_n \left| \left(d_{n-\Delta} = \phi_m\right) \right. &= w_n^{\Delta *}\left(\phi_m + i_{n-\Delta} + n_{n-\Delta}\right) + \sum_{l=0,\neq\Delta}^{L-1} w_n^{l*} x_{n-l} \\ &= \underbrace{w_n^{\Delta *}\phi_m}_{Deterministic} + \underbrace{w_n^{\Delta *}\left(i_{n-\Delta} + n_{n-\Delta}\right) + \sum_{\substack{l=0 \\ l\neq\Delta}}^{L-1} w_n^{l*} x_{n-l}}_{Random} \end{aligned} \tag{4.3}$$

The processes that enter the equalizer are all zero mean. We also assume that the deviation of the weight vector from the steady state value is negligible. Under these two assumptions, we approximate the conditional mean of $f\left(y_n \middle| d_{n-\Delta} = \phi_m\right)$ as:

$$\begin{aligned} \mathrm{E}\left[y_n \middle| \left(d_{n-\Delta} = \phi_m\right)\right] &= \mathrm{E}\left[w_n^{\Delta *}\phi_m + w_n^{\Delta *}\left(i_{n-\Delta} + n_{n-\Delta}\right) + \sum_{l=0,\neq\Delta}^{L-1} w_n^{l *} x_{n-l} \right] \\ &= w_{ss}^{\Delta *}\mathrm{E}\left[\phi_m\right] + w_{ss}^{\Delta *}\mathrm{E}\left[i_{n-\Delta}\right] + w_{ss}^{\Delta *}\mathrm{E}\left[n_{n-\Delta}\right] + \sum_{\substack{l=0 \\ l\neq\Delta}}^{L-1} w_{ss}^{l\ *}\mathrm{E}\left[x_{n-l}\right] \\ &= w_{ss}^{\Delta *}\phi_m \end{aligned} \tag{4.4}$$

Next we assume that $f\left(y_n \middle| d_{n-\Delta} = \phi_m\right)$ follows a Gaussian distribution, so that we need only the mean and the variance to describe it completely. The mean of the distribution is already derived in (4.4). For the Wiener filter we were able to assume that the output was composed of three independent components and we derived the Gaussian Mixture model in Section 2.2. However, when we tried a similar approach – the Gaussian Mixture with Steady State Weights model – this did not work very well for the NLMS equalizer as described in the previous chapter. This indicates that the assumption of independence is not a correct one. We will pursue an alternate approach to estimate the conditional variance of $f\left(y_n \middle| d_{n-\Delta} = \phi_m\right)$.

The basic definition of MSE is mean of the sum of the error squares where the error is the difference between the output and the desired signal. Thus, for *N* observations, MSE can be written as:

$$\begin{aligned} MSE &= \frac{1}{N}\sum_{n=1}^{N}\left(y_n - d_n\right)^*\left(y_n - d_n\right) \\ &= \frac{1}{N}\sum_{n=1}^{N}\left(y_n - \phi_n\right)^*\left(y_n - \phi_n\right) \end{aligned} \tag{4.5}$$

Our desired signal consists simply of the transmitted symbols. We have a closed form estimate of this MSE which is expressed in (4.1). However, J described in (4.1) is centered on the symbol values whereas, our variable of interest $f\left(y_n \middle| d_{n-\Delta} = \phi_m\right)$ is

centered on a shifted mean which is evaluated in (4.4). We compensate for this shift and obtain an estimate of the variance which is given by:

$$Var\left(f\left(y_n \left| d_{n-\Delta} = \phi_m \right. \right) \right) = J - \xi^* \xi \tag{4.6}$$

where $\xi = \phi_m - w_{ss}^{\Delta *} \phi_m$.

Combining (4.4) and (4.6) we get the PDF of $f\left(y_n \left| d_{n-\Delta} = \phi_m \right. \right)$, which is the Gaussian Model using Mean Square Error (GMMSE):

$$f\left(y_n \left| d_{n-\Delta} = \phi_m \right. \right) \sim CN\left(w_{ss}^{\Delta *} \phi_m, J - \xi^* \xi \right) \tag{4.7}$$

In the next section, we compare the BER predicted by the GMMSE model with the observed values as well as with the BER predicted by the GSMSSW model.

4.3 Simulation Results

We use the same simulation scheme as we have used before – in Sections 2.5 and 3.4 – which makes the transmitted QPSK symbols our desired signal d_n and the narrowband interference is represented by a complex sinusoid, as in (2.12).

Figure 4-1 compares the performance of the GMSE BER model and the GMSSW BER model with the observed BER values as a function of μ. The equalizer length L is taken to be 5 with SNR = 25 dB, ISR = 20 dB, and $f_i = 1/e$.

From Figure 4-1 we see that the GMSE model is able to model the BER behavior for low to medium step sizes $\left(\mu < 0.4 \right)$. The performance of the GMSE model is indeed better than with the GSMSSW model for that region. However, for larger step sizes, the GMSE is not able to capture the non-Wiener characteristics of the NLMS filter.

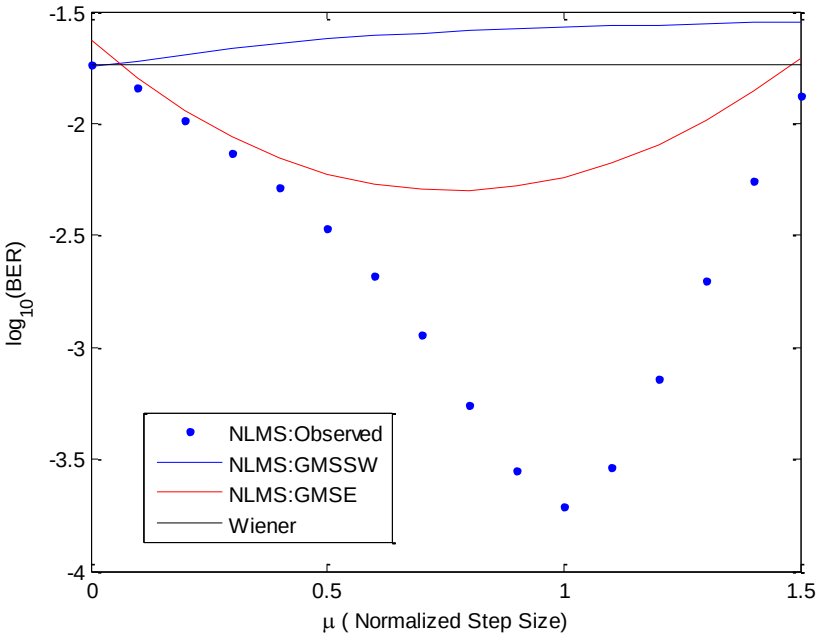

Figure 4-1. Comparison between observed and modeled, GMSSW and GMSE, BER for L = 5 as a function of μ.

Figure 4-2 shows the comparison of observed and modeled BER obtained from the GMSSW and GMSE BER models as a function SNR. A step size of $\mu = 1$ is chosen. All other parameters, i.e. SNR, ISR and f_i, are kept the same as those used to generate Figure 4-1.

Figure 4-2 shows that for a SNR less than 15 dB the GMSE modeled BER is quite accurate and the performance is significantly better than for the GMSSW model. However, for high SNR cases the GMSE model is unable to capture the non-Wiener characteristics of the NLMS equalizer. In the next section, we will investigate why the GMMSE model is working well for some cases and deteriorating in performance for other cases.

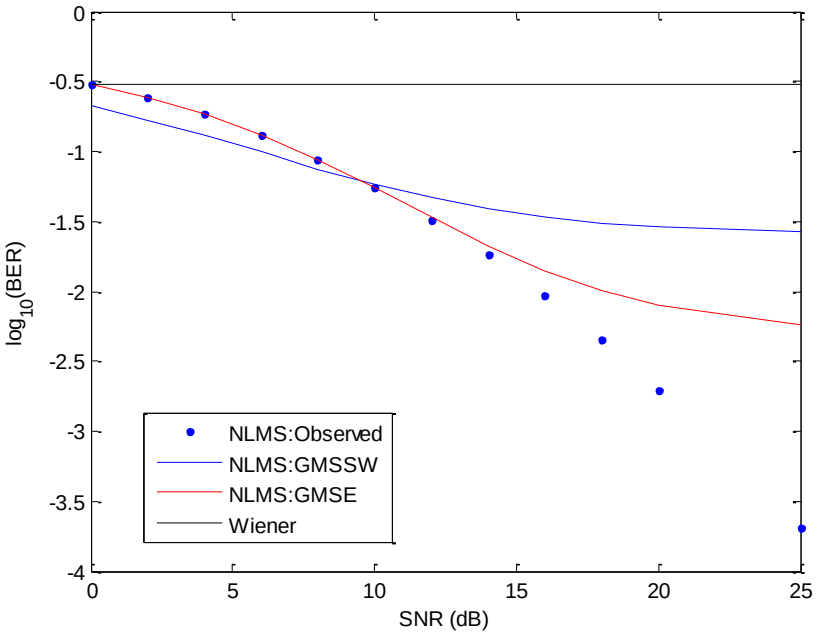

Figure 4-2. Comparison between observed and modeled, GMSSW and GMSE, BER for L = 5 as a function of SNR.

4.4 Discussion

We analyze the conditional output $f\left(y_n \middle| d_{n-\Delta} = \phi_m\right)$ for different step sizes with the equalizer length set to $L = 3$. The other parameters of importance are set as follows: SNR = 25 dB, ISR = 20 dB, and $f_i = 1/e$. Figure 4-3 shows the conditional output $f\left(y_n \middle| d_{n-\Delta} = \phi_m\right)$ for different step sizes.

From Figure 4-3 (a) we see distinct blobs in the output. The GMSE model for this case is not very accurate as we see in Figure 4-1. However, the GMSSW model is able to model this pretty effectively. This is not surprising as GMSE tries to replace the individual Gaussian components by a single Gaussian; the latter mismatch can certainly cause inaccuracies.

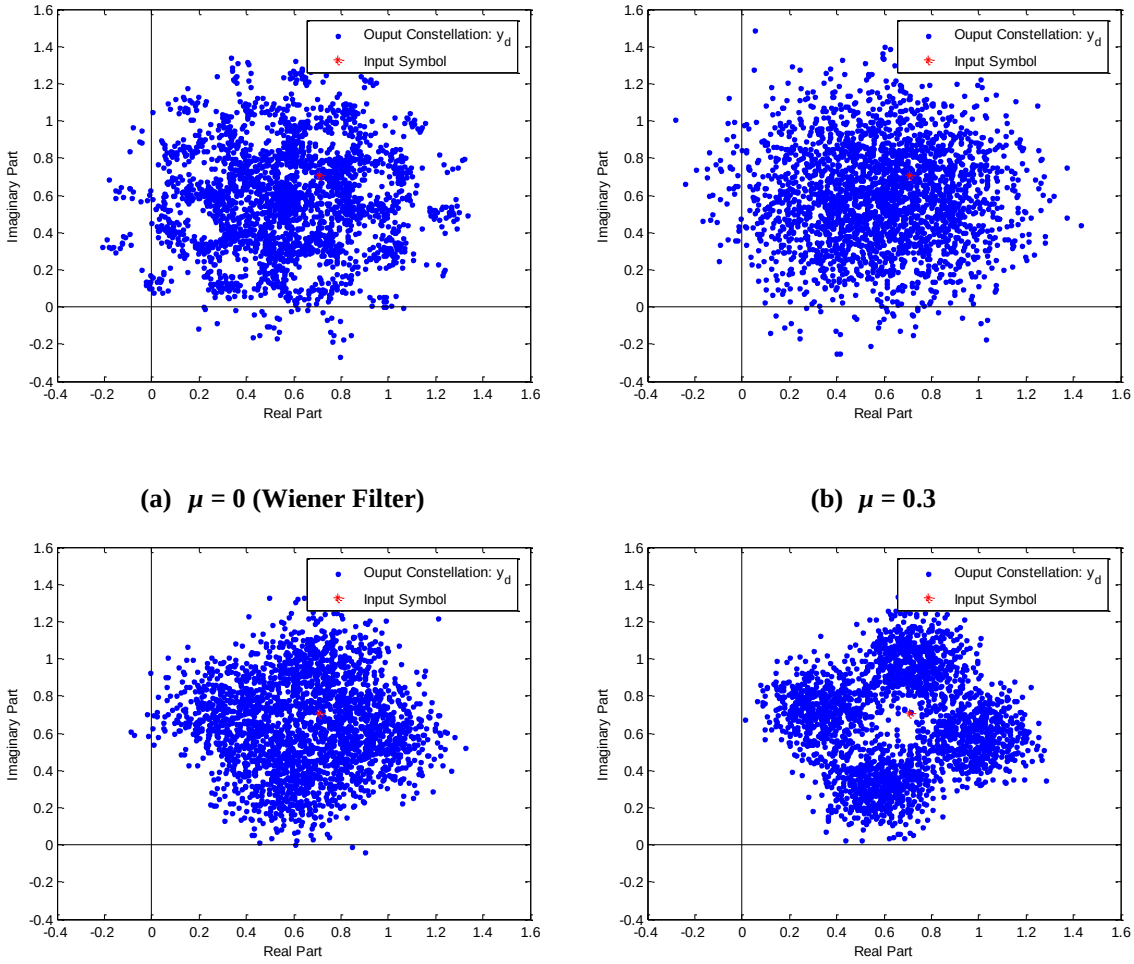

(a) μ = 0 (Wiener Filter) **(b) μ = 0.3**

(c) μ = 0.7 **(d) μ = 1**

Figure 4-3. Conditional output component for L = 5 for four different step sizes.

In Figure 4-3 (b) we notice a distinct difference from the previous case. The conditional output no longer seems to consist of distinct blobs. Instead it looks like a single Gaussian function. The simulation results corroborate this claim since the GMSE model predicts the BER much more accurately than the GMSSW model, and the assumption that the output can be represented by a single Gaussian is pretty accurate in this case.

We observe an interesting phenomenon in Figure 4-3 (c). The shape of the output component can no longer be claimed to be circular, i.e. equally distributed along both axes. We can clearly observe a non-circular behavior for $\mu = 0.7$. This non-circular

behavior is even more prominent in Figure 4-3 (d), where we observe that the output is formed by four different clusters. Naturally the assumption of the GMSE model that the output can be represented by a single Gaussian is no longer valid, which is reflected in the simulation results in Figure 4-1. Thus, from analyzing Figure 4-3, we have some insight into why the GMSE model failed to work for higher step sizes.

Figure 4-4 (a-d) show the output component for different SNR values for an equalizer length $L = 3$, step size $\mu = 1$, and an ISR = 20 dB.

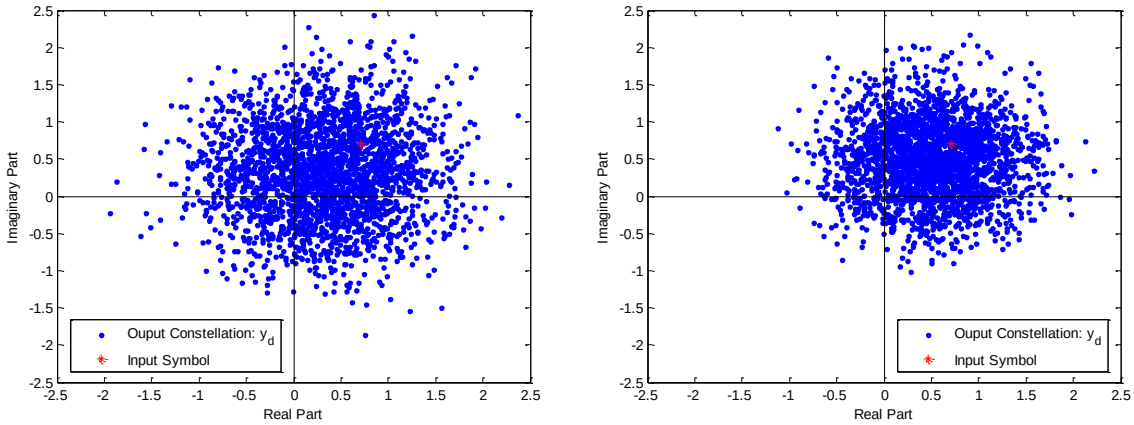

(a) SNR = 0 dB **(b) SNR = 5 dB**

(c) SNR = 15 dB **(d) SNR = 25 dB**

Figure 4-4. Conditional output component for *L* = 5 for four different SNR.

Figures 4-4 (a-b) show that for high SNR values the conditional output component can be represented by a single Gaussian. This is because the Gaussian white noise power is very high and hence that component dominates in the output. As a result we observe in Figure 4.2 that the GMMSE model for BER produces a pretty accurate prediction.

For Figures 4-4 (c-d) we see that the output shows non-circular behavior, just as we saw in Figures 4-3 (c-d). As expected, the GMSE model for BER does not provide accurate predictions. An interesting thing to note in this context is that in Figures 4-3 (d) and 4-4 (d) we observe that the output is composed of four blobs. The number four represents the number of possible symbols in a QPSK modulation scheme. Although we have observed this behavior, a comprehensive mathematical model explaining why the equalizer output behaves the way it does – for high step sizes – is yet to be formulated.

4.5 Summary

In this chapter we introduced a new model to estimate the BER for an adaptive NLMS equalizer – the GMSE BER model. This model was able to capture the non-Wiener behavior of the NLMS equalizer for a certain range of step sizes $(\mu < 0.4)$. However, for higher step sizes, the GMSE model failed to model the non-Wiener behavior. At best, we can say that the GMSE model provides us with a very conservative upper bound for higher step sizes.

CHAPTER 5 CONCLUSIONS

5.1 Conclusions

This work focused on the BER characteristics of the adaptive NLMS equalizer in an environment where a narrowband sinusoidal interference is dominant. The goal of this work was to develop analytical models which can predict the BER performance of such an equalizer for the particular scenario.

We started by deriving the BER model for a Wiener equalizer constrained to have the FIR structure, as this is a simple and usual structure for adaptive equalization. Based on observations of the behavior of signal components for the case of the FIR Wiener equalizer, the Gaussian Mixture (GM) model was hypothesized for the prediction of BER. The GM model predicted the BER behavior pretty accurately, but it was computationally complex for larger equalizers. To address the latter issue, a computationally simple Gaussian model was proposed; potentially sacrificing accuracy of BER prediction for computational simplicity. However, for larger equalizers (equalizers with a larger number – in the tens – of taps) the accuracy of the model was not affected substantially compared to the reduction achieved in computational complexity.

With the BER model for the FIR Wiener equalizer in place, to serve as a suitable benchmark, we proceeded towards developing similar BER models for adaptive NLMS equalizers. We introduce the Gaussian Mixture with Steady State Weights model (GMSSW) model as a logical extension of the GM model, the only difference being that the Wiener weights were replaced by the steady state NLMS weights. The simulation performance showed that the GMSSW model is unable to capture the non-Wiener characteristics of the adaptive NLMS equalizer. A thorough analysis of individual signal components provided insight as to why the GMSSW model failed to work for the adaptive case and highlighted the primary difference between the adaptive NLMS equalizer and its Wiener counterpart. The residual interference component at the output was different in those two cases. While, the Wiener equalizer focused only on mitigating

the interference in terms of MSE, the NLMS equalizer actually exploited the narrowband interference to its advantage.

As a result, an improved BER model – the Gaussian using Mean Square Error Model (GMSE) – was introduced for the NLMS equalizer, in which the steady state Mean Square Error for the NLMS equalizer is used. The simulation results show that the GMSE model was able to capture the non-Wiener characteristics for certain cases while failing for others. The following table summarizes the BER modeling work to date.

Table 5-1. Applicability of the Different BER Models for Different Scenarios.

Step Size (μ)	**Low SNR (< 15 dB)**	**High SNR (> 20 dB)**
Small (< 0.1)	GMSSW	GMSE
Medium (0.1 – 0.4)	GMSE	GMSE
Large (0.4 – 1)	GMSE	To Be Done

5.2 Future Work

One of the possible future directions which is evident from Table 5.1 is to find an appropriate BER model which accurately estimates the BER for large step sizes. It is to be noted here that in an environment dominated by a narrowband interference large step sizes yield the best performance in terms of BER. A model that is able to explain the BER performance in that region is consequently of much importance and will help to explain the non-Wiener characteristics of the NLMS equalizer in greater detail. From a practical point of view, such a model can be used to indicate when the NLMS equalizer should use a large step-size.

Another possible avenue for extension of this research is to develop similar BER models for different scenarios. Different scenarios can range from multiple narrowband

interferers, taking into account imperfect synchronization, non-sinusoidal narrowband interference, and so on.

REFERENCES

[1] J. G. Proakis and M. Salehi, *Digital Communications*, 5th ed.: McGraw-Hill, 2008.

[2] R. W. Lucky, "Techniques for adaptive equalization of digital communication systems," *Bell System Technical Journal, The*, vol. 45, pp. 255-286, 1966.

[3] B. Widrow, P. E. Mantey, L. J. Griffiths, and B. B. Goode, "Adaptive antenna systems," *Proceedings of the IEEE*, vol. 55, pp. 2143-2159, 1967.

[4] J. G. Proakis and J. Miller, "An adaptive receiver for digital signaling through channels with intersymbol interference," *Information Theory, IEEE Transactions on*, vol. 15, pp. 484-497, 1969.

[5] S. U. H. Qureshi, "Adaptive equalization," *Proceedings of the IEEE*, vol. 73, pp. 1349-1387, 1985.

[6] L. B. Milstein, "Interference rejection techniques in spread spectrum communications," *Proceedings of the IEEE*, vol. 76, pp. 657-671, 1988.

[7] J. D. Laster and J. Reed, "Interference rejection in digital wireless communications," *Signal Processing Magazine, IEEE*, vol. 14, pp. 37-62, 1997.

[8] H. V. Poor, "Active interference suppression in CDMA overlay systems," *Selected Areas in Communications, IEEE Journal on*, vol. 19, pp. 4-20, 2001.

[9] A. Batra, "Mitigation Techniques for Severe Narrowband Interference," Ph. D., UC San Diego, 2009.

[10] R. C. North, R. A. Axford, and J. R. Zeidler, "The performance of adaptive equalization for digital communication systems corrupted by interference," in *Signals, Systems and Computers, 1993. 1993 Conference Record of The Twenty-Seventh Asilomar Conference on*, 1993, pp. 1548-1553 vol.2.

[11] S. Haykin, *Adaptive Filter Theory*, 5th ed.: Prentice Hall, 2013.

[12] M. Reuter and B. Zeidler, "Non-Wiener effects in LMS-implemented adaptive equalizers," in *Acoustics, Speech, and Signal Processing, 1997. ICASSP-97., 1997 IEEE International Conference on*, 1997, pp. 2509-2512 vol.3.

[13] K. J. Quirk, J. R. Zeidler, and L. B. Milstein, "Bounding the performance of the LMS estimator for cases where performance exceeds that of the finite Wiener

filter," in *Acoustics, Speech and Signal Processing, 1998. Proceedings of the 1998 IEEE International Conference on*, 1998, pp. 1417-1420 vol.3.

[14] M. Reuter and J. R. Zeidler, "Nonlinear effects in LMS adaptive equalizers," *Signal Processing, IEEE Transactions on*, vol. 47, pp. 1570-1579, 1999.

[15] M. Reuter, K. Quirk, B. Zeidler, and L. Milstein, "Non-linear effects in LMS adaptive filters," in *Adaptive Systems for Signal Processing, Communications, and Control Symposium 2000. AS-SPCC. The IEEE 2000*, 2000, pp. 141-146.

[16] A. A. Beex and J. R. Zeidler, "Data structure and non-linear effects in adaptive filters," in *Digital Signal Processing, 2002. DSP 2002. 2002 14th International Conference on*, 2002, pp. 659-662 vol.2.

[17] A. A. Beex and J. R. Zeidler, "Non-Wiener effects in recursive least squares adaptation," in *Signal Processing and Its Applications, 2003. Proceedings. Seventh International Symposium on*, 2003, pp. 595-598 vol.2.

[18] A. A. Beex and J. R. Zeidler, "Linking sequence behavior in ANC," in *Acoustics, Speech, and Signal Processing, 2004. Proceedings. (ICASSP '04). IEEE International Conference on*, 2004, pp. ii-833-6 vol.2.

[19] T. Ikuma, A. A. Beex, and J. R. Zeidler, "Non-Wiener Weight Behavior of LMS Transversal Equalizers," in *Acoustics, Speech and Signal Processing, 2007. ICASSP 2007. IEEE International Conference on*, 2007, pp. III-1297-III-1300.

[20] H. J. Butterweck, "Iterative analysis of the steady-state weight fluctuations in LMS-type adaptive filters," *Signal Processing, IEEE Transactions on*, vol. 47, pp. 2558-2561, 1999.

[21] T. Ikuma, A. A. Beex, and J. R. Zeidler, "Non-Wiener Mean Weight Behavior of LMS Transversal Equalizers With Sinusoidal Interference," *Signal Processing, IEEE Transactions on*, vol. 56, pp. 4521-4525, 2008.

[22] T. Ikuma and A. A. Beex, "Improved Mean-Square Error Estimate for the LMS Transversal Equalizer With Narrowband Interference," *Signal Processing, IEEE Transactions on*, vol. 56, pp. 5273-5277, 2008.

[23] T. Ikuma, "Non-Wiener Effects in Narrowband Interference Mitigation Using Adaptive Transversal Equalizers," Ph. D., Virginia Tech, 2007.

[24] R. A. Iltis and L. B. Milstein, "An Approximate Statistical Analysis of the Widrow LMS Algorithm with Application to Narrow-Band Interference Rejection," *Communications, IEEE Transactions on*, vol. 33, pp. 121-130, 1985.

[25] M. E. Davis and L. B. Milstein, "Anti-jamming properties of a DS-CDMA equalization filter," in *Military Communications Conference, 1993. MILCOM '93. Conference record. Communications on the Move., IEEE,* 1993, pp. 1008-1012 vol.3.

[26] A. J. Coulson, "Bit error rate performance of OFDM in narrowband interference with excision filtering," *Wireless Communications, IEEE Transactions on,* vol. 5, pp. 2484-2492, 2006.

[27] A. Leon-Garcia, *Probability, Statistics and Random Processes For Electrical Engineering,* 3rd ed.: Prentice Hall, 2008.